

GROWTH RATE OF LIQUIDITY PROVIDER'S WEALTH IN G3MS

CHEUK YIN LEE, SHEN-NING TUNG, AND TAI-HO WANG

ABSTRACT. We study how trading fees and continuous-time arbitrage affect the profitability of liquidity providers (LPs) in Geometric Mean Market Makers (G3Ms). We use stochastic reflected diffusion processes to analyze the dynamics of a G3M model [Eva21] under the arbitrage-driven market [MMRZ22a]. Our research focuses on calculating LP wealth and extends the findings of Tassy and White [TW20] related to the constant product market maker (Uniswap v2) to a wider range of G3Ms, including Balancer. This allows us to calculate the long-term expected logarithmic growth of LP wealth, offering new insights into the complex dynamics of AMMs and their implications for LPs in decentralized finance.

1. INTRODUCTION

Decentralized finance (DeFi) has revolutionized financial markets by enabling trustless trading and investment activities through blockchain technology [CJ21, GM23]. At the heart of this revolution are Automated Market Makers (AMMs) [Moh22], which replace traditional order book exchanges with smart contracts that automate price discovery and order execution. This innovation eliminates intermediaries, reduces trading costs, and enhances accessibility for a wider range of participants.

Among the diverse landscape of AMM designs, Geometric Mean Market Makers (G3Ms) have gained significant traction, powering popular DeFi protocols like Uniswap [AZR20] and Balancer [MM19]. G3Ms utilize a weighted geometric mean function to determine asset prices within their liquidity pools. This unique pricing mechanism fosters a predictable relationship between asset reserves and prices, promoting market efficiency and arbitrage resistance.

A large body of literature has extensively examined various aspects of AMM mechanics. [AKC⁺19, AC20] analyzed the theoretical properties and price-tracking capabilities of constant function markets. [Eva21] extended this analysis to G3Ms with variable weights, while [FMW23, FMW24] investigated impermanent loss and hedging strategies. The concept of "loss-versus-rebalancing" (LVR) was quantified by Milionis et al. [MMRZ22b, MMRZ22a, MMR23], who developed frameworks for measuring systematic LP losses in both standard AMMs and concentrated liquidity markets. [CDM23, CDM24] explored predictable loss in constant function markets and developed optimal liquidity provision strategies under separate fee rate models. [BEK24] analyzed risks and incentives in AMM liquidity provision, proposing novel transaction cost structures. More recently, [NTYY24] examined arbitrage-driven price dynamics in fee-based AMMs, providing insights into the relationship between fee structures and market behavior.

Date: September 9, 2025.

Key words and phrases. Automatic market making, Decentralized exchange, Decentralized finance.

Previous research has extensively examined various aspects of AMM mechanics. Angeris et al. [AKC⁺19, AC20] analyzed the theoretical properties and price-tracking capabilities of constant function markets. Evans [Eva21] extended this analysis to G3Ms with variable weights, while others like Fukasawa et al. [FMW23, FMW24] investigated impermanent loss and hedging strategies. Milionis et al. [MMRZ22b, MMRZ22a, MMR23], who quantified it as "loss-versus-rebalancing" (LVR) and developed frameworks for measuring systematic LP losses in both standard AMMs and concentrated liquidity markets.

While the existing literature provides a rich foundation for understanding AMMs, a key question remains: How do arbitrage dynamics and trading fees interact to influence the long-term growth of liquidity provider (LP) wealth in G3Ms? This paper aims to address this question by developing a novel framework for analyzing LP wealth evolution in G3Ms, extending beyond the specific case of Uniswap V2 studied in [TW20]. We model the G3M under the influence of continuous arbitrage activity in the presence of a frictionless reference market, drawing inspiration from the framework presented in [MMRZ22b, MMRZ22a, MMR23]. Our analysis leverages the theory of reflected diffusion processes to capture the dynamics of mispricing and its effect on LP returns.

This research makes three key contributions:

- (1) We derive explicit formulas for LP wealth growth rates under various market conditions, encompassing different volatility and drift scenarios.
- (2) We analyze how different fee structures affect LP returns, offering insights into the optimal design of G3Ms.
- (3) We compare the performance of G3Ms to traditional constant rebalanced portfolio strategies, highlighting the potential of G3Ms to serve as an index infrastructure within the DeFi ecosystem.

By employing reflected diffusion processes [LS84], we extend and generalize existing results on LP wealth dynamics, providing a more comprehensive and unified framework. Our findings offer valuable insights for both LPs and AMM designers, contributing to a deeper understanding of DeFi market mechanisms and their implications for investor returns.

Outline. The remainder of the paper is organized as follows. Section 2 establishes notation and examines market dynamics with and without transaction costs. Section 3 explores the arbitrageur's problem and G3M dynamics under both discrete and continuous arbitrage. Section 4 presents our main results, connecting LP wealth growth to parabolic PDEs with Neumann boundary conditions and extending results to cases with independent stochastic volatility and drift.

2. CONSTANT WEIGHT G3MS

Geometric Mean Market Makers (G3Ms) are a prominent class of automated market makers (AMMs) that utilize a weighted geometric mean to define the feasible set of trades. This section provides a detailed review of G3M mechanisms, following the work in [Eva21, Moh22, FMW24], for a system with two assets, X and Y , and a fixed weight $w \in (0, 1)$.

2.1. G3M Trading Mechanics. Let $(x, y) \in \mathbb{R}_+^2$ denote the reserves of assets X and Y in the liquidity pool (LP). The core principle of a G3M is to maintain a constant weighted geometric mean of the reserves:

$$x^w y^{1-w} = \ell, \quad (1)$$

where ℓ represents the overall liquidity in the pool.

2.1.1. Trading without Transaction Costs. In an idealized setting without transaction costs, trades in a G3M must preserve the constant weighted geometric mean of the reserves. This means a trade $\Delta = (\Delta_x, \Delta_y) \in \mathbb{R}^2$, representing the changes in asset reserves, is feasible if and only if:

$$x^w y^{1-w} = (x + \Delta_x)^w (y + \Delta_y)^{1-w}. \quad (2)$$

Here, $\Delta_x > 0$ indicates that asset X is being added to the pool, while $\Delta_x < 0$ means X is being withdrawn.

To determine the price of asset X relative to asset Y , we analyze how infinitesimal changes in reserves affect the weighted geometric mean. Taking the total derivative of equation (1), we get

$$wx^{w-1}y^{1-w}dx + (1-w)x^w y^{-w}dy = 0,$$

which simplifies to

$$w\frac{dx}{x} + (1-w)\frac{dy}{y} = 0.$$

This relationship between infinitesimal changes in x and y allows us to define the price P of asset X in terms of asset Y :

$$P = -\frac{d\Delta_y}{d\Delta_x} \Big|_{\Delta_x=0} = -\frac{dy}{dx} = \frac{y/(1-w)}{x/w} = \frac{w}{1-w} \frac{y}{x}. \quad (3)$$

Therefore, the price in a G3M without transaction costs is determined solely by the ratio of the reserves.

Remark 2.1. A key advantage of G3Ms without transaction costs is their *path independence* [AC20, §2.3]. This means the final state of the pool depends only on the net change in reserves, not the specific sequence of trades that led to it. This property makes these G3Ms resistant to price manipulation strategies.

2.1.2. With Transaction Costs. In a more realistic scenario, there are transaction costs, typically modelled as a proportional fee. Let $\gamma \in (0, 1)$ represent the transaction cost parameter, where $1 - \gamma$ is the proportional fee. The trading process now involves two key concepts: feasible trades and reserve updates.

Determining Feasible Trades. A trade is feasible if it satisfies the following conditions, which incorporate the transaction cost:

- **Buying Asset X from the Pool ($\Delta_y > 0$):** The trader pays a fee on the amount of asset Y they provide.

$$(x + \Delta_x)^w (y + \gamma\Delta_y)^{1-w} = \ell. \quad (4)$$

- **Selling Asset X to the Pool ($\Delta_x > 0$):** The trader pays a fee on the amount of asset X they provide.

$$(x + \gamma\Delta_x)^w (y + \Delta_y)^{1-w} = \ell. \quad (5)$$

Updating Reserves. After a trade, the reserves and the pool's liquidity are updated accordingly:

$$\begin{aligned} x &\mapsto x + \Delta_x, \\ y &\mapsto y + \Delta_y, \\ \ell &\mapsto (x + \Delta_x)^w (y + \Delta_y)^{1-w}. \end{aligned}$$

Introducing transaction costs leads to several important differences:

Marginal Exchange Rate. The effective price for infinitesimal trades is given by the marginal exchange rate, which now incorporates the transaction cost.

- For buying X : Differentiating (4) gives $-\frac{d\Delta_y}{d\Delta_x}|_{\Delta_x=0} = \frac{1}{\gamma}P$.
- For selling X : Differentiating (5) gives $-\frac{d\Delta_y}{d\Delta_x}|_{\Delta_x=0} = \gamma P$.

This creates a **bid-ask spread**, where the price for buying X is higher than the price for selling X .

Constant Wealth Proportion. Despite the transaction costs, the proportion of asset X (and Y) in the pool's total wealth remains constant at w (and $1-w$, respectively), as shown by (3):

$$\frac{Px}{w} = \frac{y}{1-w}. \quad (6)$$

Relationship between Reserves and Liquidity. There is a correspondence between (x, y) and (ℓ, P) given by:

$$\begin{aligned} \ln x &= \ln \ell - (1-w) \ln P - (1-w) \ln(1-w) + (1-w) \ln w, \\ \ln y &= \ln \ell + w \ln P + w \ln(1-w) - w \ln w. \end{aligned}$$

Price Impact of Trading. The impact of trading on the pool price is given by:

$$\frac{dP}{P} = \frac{dy}{y} - \frac{dx}{x} = -\frac{1}{1-w} \frac{dx}{x} = \frac{1}{w} \frac{dy}{y}.$$

Remark 2.2.

- (1) The transaction cost parameter γ creates a bid-ask spread, similar to traditional limit order books, where buyers pay a slightly higher price than sellers.
- (2) Unlike G3Ms without transaction fees, the presence of transaction costs introduces **path dependence** [AC20, §2.3]. This means that the order and size of trades influence the final outcome. To illustrate this, consider a trader selling Δ_x of asset X in exchange for Δ_y of asset Y . The transaction satisfies

$$(x + \gamma \Delta_x)^w (y + \Delta_y)^{1-w} = x^w y^{1-w}.$$

If the trader instead splits the trade into two smaller transactions, $\Delta_x = \Delta_x^1 + \Delta_x^2$, receiving Δ_y^1 and Δ_y^2 of asset Y respectively, then the trades satisfy

$$\begin{aligned} (x + \gamma \Delta_x^1)^w (y + \Delta_y^1)^{1-w} &= x^w y^{1-w}, \\ (x + \Delta_x^1 + \gamma \Delta_x^2)^w (y + \Delta_y^1 + \Delta_y^2)^{1-w} &= (x + \Delta_x^1)^w (y + \Delta_y^1)^{1-w}. \end{aligned}$$

Comparing these equations reveals that $\Delta_y < \Delta_y^1 + \Delta_y^2 < 0$, demonstrating that splitting the trade leads to a higher cost (i.e., a smaller amount of asset Y received). This phenomenon is further explored in [AKC⁺19, Appendix D] and [FMW24, Proposition 1].

2.2. Continuous Trading Dynamics. In the continuous trading regime, where trades occur infinitesimally often, we can describe the G3M dynamics using differential equations. These equations capture how the reserves, price, and liquidity evolve in response to continuous buying and selling.

2.2.1. Reserve Dynamics. The changes in reserves x and y are governed by the following equations, which incorporate the transaction cost parameter γ :

- **When buying X from the pool ($dx < 0$):**

$$w \frac{dx}{x} + \gamma(1-w) \frac{dy}{y} = 0. \quad (7)$$

- **When selling X to the pool ($dx > 0$):**

$$\gamma w \frac{dx}{x} + (1-w) \frac{dy}{y} = 0. \quad (8)$$

These equations reflect that when buying X , the trader pays a fee on the Y asset provided, while when selling X , the fee is paid on the X asset provided.

2.2.2. Price Dynamics. The price P of asset X relative to asset Y evolves according to:

$$\frac{dP}{P} = \frac{dy}{y} - \frac{dx}{x} = \begin{cases} (1 + \gamma \frac{1-w}{w}) \frac{dy}{y} & \text{if } dy > 0, \\ (1 + \frac{1}{\gamma} \frac{1-w}{w}) \frac{dy}{y} & \text{if } dy < 0. \end{cases} \quad (9)$$

This equation shows how buying pressure ($dy > 0$) pushes the price up while selling pressure ($dy < 0$) pushes it down. The transaction cost γ affects the magnitude of these price changes.

2.2.3. Liquidity Dynamics. The liquidity ℓ of the pool changes as follows:

$$\frac{d\ell}{\ell} = w \frac{dx}{x} + (1-w) \frac{dy}{y} = \begin{cases} (1 - \gamma)(1-w) \frac{dy}{y} & \text{if } dy > 0, \\ (1 - \frac{1}{\gamma})(1-w) \frac{dy}{y} & \text{if } dy < 0. \end{cases} \quad (10)$$

This equation reveals that the liquidity consistently increases due to the transaction costs collected by the pool.

Remark 2.3. In the continuous trading regime, the G3M effectively maintains certain quantities constant, depending on the direction of trading:

- When buying X : $x^w y^{\gamma(1-w)}$ remains constant.
- When selling X : $x^{\gamma w} y^{1-w}$ remains constant.

This behavior leads to a continuous accumulation of liquidity in the pool.

2.3. LP Wealth. The wealth of a liquidity provider (LP) in a G3M is determined by the value of their holdings in the pool. At any given time, the LP's wealth, denoted by $V(P)$, is simply the sum of the value of their X holdings and their Y holdings: $V(P) = Px + y$ where P is the current price of asset X relative to asset Y .

Using the relationship between the reserves, price, and liquidity (equation (6)), we can express the LP's wealth in a more convenient form:

$$V(P) = \frac{Px}{w} = \frac{Px}{w} \left(\frac{\frac{Px}{w}}{\frac{Px}{w}} \right)^w \left(\frac{\frac{y}{1-w}}{\frac{Px}{w}} \right)^{1-w} = \frac{\ell P^w}{w^w (1-w)^{1-w}}. \quad (11)$$

This equation shows that the LP's wealth is directly proportional to the pool's liquidity ℓ and depends on the price P raised to the power of the weight w . Taking the logarithm of both sides, we obtain the log wealth:

$$\ln V(P) = \ln \ell + w \ln P + \mathcal{S}_w, \quad (12)$$

where $\mathcal{S}_w = -w \ln w - (1-w) \ln (1-w)$. The term \mathcal{S}_w is the entropy of the weight distribution $(w, 1-w)$, which reflects the diversification of the LP's holdings.

Remark 2.4. The LP's wealth is expressed here in terms of the G3M pool price P . This is natural from the LP's perspective, as they may not always have access to the true reference market price. Furthermore, this formulation (equation (12)) is crucial for computing the long-term growth rate of LP wealth.

Section 3.3 compares this approach to a valuation based on the reference market price. This analysis will show that the logarithmic values of these two expressions differ by, at most, a constant factor, which depends on the transaction cost parameter γ .

3. ARBITRAGE-DRIVEN G3M DYNAMICS

This section investigates how the presence of arbitrageurs influences the behavior of a G3M. Arbitrageurs are traders who exploit price discrepancies between different markets to profit. In our context, they take advantage of any differences between the G3M pool price and the price on an external reference market.

To focus specifically on the impact of arbitrage, we make two simplifying assumptions:

Assumption 3.1. There are no noise traders in the market.

Noise traders are those who trade based on non-fundamental factors, introducing randomness into the market. By excluding them, we can isolate the effects of arbitrageurs who act rationally based on price discrepancies.

Assumption 3.2. There exists an external reference market with infinite liquidity and no trading costs.

This assumption ensures that arbitrageurs can execute trades in the reference market without incurring any costs or affecting the market price. This idealized setting allows us to focus on the arbitrageurs' impact on the G3M.

3.1. Arbitrage Bounds and Price Dynamics. In the presence of a frictionless external reference market (Assumption 3.2), arbitrageurs can freely exploit any price discrepancies between the G3M and the reference market. This arbitrage activity imposes bounds on the G3M price, preventing it from straying too far from the reference market price.

To understand these bounds, let's denote the price of asset X relative to asset Y in the reference market as S , and the corresponding price in the G3M pool as P . Arbitrageurs aim to maximize their profit by buying asset X where it's cheaper and selling it where it's more expensive. This leads to the following optimization problem for an arbitrageur, as shown in [AKC⁺19]:

$$\begin{aligned} \max_{\Delta \in \mathbb{R}^2} & - (S\Delta_x + \Delta_y) \\ \text{s.t. } & (x_0 + \gamma\Delta_x)^w (y_0 + \Delta_y)^{1-w} = x_0^w y_0^{1-w} \quad \text{if } \Delta_x \geq 0 \\ & (x_0 + \Delta_x)^w (y_0 + \gamma\Delta_y)^{1-w} = x_0^w y_0^{1-w} \quad \text{if } \Delta_x < 0, \end{aligned} \tag{13}$$

where (x_0, y_0) represents the initial reserve of assets X and Y in the pool. This optimization problem captures the arbitrageur's objective: maximize profit while adhering to the G3M's trading rules (equations (4) and (5)), which include transaction costs.

The solution to this optimization problem reveals that the G3M price, after arbitrageurs have acted, must satisfy

$$P^* = \begin{cases} \gamma^{-1}S & \text{if } P_0 > \gamma^{-1}S, \\ P_0 & \text{if } \gamma S \leq P_0 \leq \gamma^{-1}S, \\ \gamma S & \text{if } P_0 < \gamma S. \end{cases}$$

where γ is the transaction cost parameter of the G3M [AKC⁺19, §2.1]. This interval, $[\gamma S, \gamma^{-1}S]$, defines the *no-arbitrage bounds*.

Essentially, these bounds create a "safe zone" for the G3M price. If the price falls outside this zone, arbitrageurs will immediately execute trades, buying or selling asset X until the price returns within the bounds. This arbitrage activity effectively regulates the G3M price, keeping it anchored to the reference market price.

Figure 1 provides empirical evidence of this behavior. It shows a time series of the G3M price, clearly demonstrating that it consistently stays within the no-arbitrage bounds.

3.2. Mispicing and Arbitrage Dynamics. To formally analyze how arbitrageurs influence the G3M's behavior, we introduce the concept of **mispicing**, which quantifies the discrepancy between the G3M pool price and the reference market price. We investigate how this mispricing evolves under both discrete and continuous arbitrage scenarios, building upon the framework in [MMRZ22a, MMR23].

3.2.1. Discrete Arbitrage Model. First, we consider a discrete-time model where arbitrageurs arrive at discrete times:

Assumption 3.3. Arbitrageurs arrive at discrete times $0 = \tau_0 < \tau_1 < \tau_2 < \dots < \tau_m \leq T$.

At each arrival time τ_i , an arbitrageur observes the reference market price S_{τ_i} and the prevailing G3M pool price $P_{\tau_{i-1}}$. They then execute trades to exploit any price difference, aiming to maximize their profit.

To quantify this price difference, we define the mispricing Z_t as:

$$Z_t \triangleq \ln \frac{S_t}{P_t}. \quad (14)$$

This quantity measures the logarithmic difference between the reference market price S_t and the G3M pool price P_t .

Following the discussion of Section 3.1, the arbitrage process can be described by the following recipe, similar to [MMR23, Lemma 2]:

- **If the G3M price is too low relative to the reference market** ($S_{\tau_i} < \gamma P_{\tau_{i-1}}$ or equivalently $Z_{\tau_i^-} < \ln \gamma$), the arbitrageur sells asset X to the pool at the relatively higher price and simultaneously buys it on the reference market at the lower price. This pushes the G3M price up until it reaches the upper no-arbitrage bound ($Z_{\tau_i} = \ln \gamma$).
- **If the G3M price is too high relative to the reference market** ($S_{\tau_i} > \gamma^{-1} P_{\tau_{i-1}}$ or equivalently $Z_{\tau_i^-} > -\ln \gamma$), the arbitrageur buys asset X from the pool at the relatively cheaper price and immediately sells it on the reference market at the higher price. This arbitrage activity pushes the G3M price down until it reaches the lower no-arbitrage bound ($Z_{\tau_i} = -\ln \gamma$).
- **If the G3M price is already within the no-arbitrage bounds** ($\gamma P_{\tau_{i-1}} \leq S_{\tau_i} \leq \gamma^{-1} P_{\tau_{i-1}}$ or equivalently $\ln \gamma \leq Z_{\tau_i^-} \leq -\ln \gamma$), there is no profitable arbitrage opportunity, and the arbitrageur does not execute any trades.

This arbitrage process leads to the following update rule for the G3M price at each arbitrageur arrival time:

$$P_{\tau_i} = \begin{cases} \gamma S_{\tau_i} & \text{if } Z_{\tau_i^-} < \ln \gamma, \\ P_{\tau_{i-1}} & \text{if } \ln \gamma \leq Z_{\tau_i^-} \leq -\ln \gamma, \\ \gamma^{-1} S_{\tau_i} & \text{if } Z_{\tau_i^-} > -\ln \gamma. \end{cases} \quad (15)$$

Accordingly, the mispricing process evolves as:

$$\begin{aligned} Z_{\tau_i} &= \max \left\{ \min \{Z_{\tau_i^-}, -\ln \gamma\}, \ln \gamma \right\} \\ &= \begin{cases} \ln \gamma & \text{if } Z_{\tau_i^-} < \ln \gamma, \\ Z_{\tau_i^-} & \text{if } \ln \gamma \leq Z_{\tau_i^-} \leq -\ln \gamma, \\ -\ln \gamma & \text{if } Z_{\tau_i^-} > -\ln \gamma. \end{cases} \end{aligned} \quad (16)$$

These equations capture how arbitrageurs adjust the G3M price in discrete steps to keep it within the no-arbitrage bounds.

Proposition 3.4 (Discrete Mispicing Dynamics). *Given Assumptions 3.1, 3.2, and 3.3 and the initial condition $\gamma P_0 \leq S_0 \leq \gamma^{-1} P_0$, we can define:*

$$J_i = \max \left\{ \min \{Z_{\tau_i^-}, -\ln \gamma\}, \ln \gamma \right\} - Z_{\tau_i^-}, \quad L_t = \sum_{i:\tau_i \leq t} \{J_i\}^+, \quad U_t = \sum_{i:\tau_i \leq t} \{J_i\}^-,$$

where $\{a\}^+ = \max\{a, 0\}$ and $\{a\}^- = \max\{-a, 0\}$ denote the positive and negative parts of a , respectively. Then for all $t \geq 0$,

$$\begin{aligned}\ln P_t &= \ln P_0 + U_t - L_t, \\ Z_t &= \ln S_t - \ln P_0 + L_t - U_t.\end{aligned}$$

Moreover, L_t and U_t satisfy:

$$L_t = \sup_{i: \tau_i \leq t} (-\ln(\gamma P_0) + \ln S_{\tau_i} - U_{\tau_i})^-, \quad (17)$$

$$U_t = \sup_{i: \tau_i \leq t} (\ln(\gamma^{-1} P_0) - \ln S_{\tau_i} - L_{\tau_i})^-. \quad (18)$$

Proof. The first assertion follows directly from (15) and (16). For the second assertion, note that both sides of (17) and (18) are non-decreasing and piecewise constant, with potential jumps occurring at τ_i for $0 \leq i \leq m$. It suffices to show the equalities at each τ_i .

The proof employs induction on i . For $i = 0$, the equalities hold by the initial condition $\ln \gamma \leq Z_0 \leq -\ln \gamma$. For $i < k$, the induction hypothesis yields:

$$L_{\tau_k} = \max \{L_{\tau_{k-1}}, \{-\ln \gamma + Z_{\tau_k} - L_{\tau_k}\}^-\}.$$

Given that

$$L_{\tau_k} \begin{cases} \geq L_{\tau_{k-1}} & \text{if } Z_{\tau_k} = \ln \gamma, \\ = L_{\tau_{k-1}} & \text{otherwise,} \end{cases}$$

it follows that

$$\{-\ln \gamma + Z_{\tau_k} - L_{\tau_k}\}^- = \min\{L_{\tau_k} + \ln \gamma - Z_{\tau_k}, 0\} \begin{cases} = L_{\tau_{k-1}} & \text{if } Z_{\tau_k} = \ln \gamma, \\ < L_{\tau_{k-1}} & \text{otherwise,} \end{cases}$$

which validates (17). The same argument confirms (18). \square

Remark 3.5.

- The processes L_t and U_t act as **regulatory barriers** on the mispricing process Z_t . Specifically, at each arbitrage time τ_i , L_t prevents Z_t from falling below the lower bound $\ln \gamma$, while U_t prevents it from exceeding the upper bound $-\ln \gamma$. This ensures that the mispricing remains within the no-arbitrage interval $[\ln \gamma, -\ln \gamma]$.
- Fukasawa et al. [FMW23, FMW24] analyzed arbitrage in G3Ms by focusing on the dynamics of the reserve processes. Here, we adopt a different perspective by directly analyzing the mispricing process, which is compatible with their work through Equation (6). Our approach has the advantage of analyzing the growth rate of liquidity provider wealth, as discussed in Section 4.

3.2.2. Continuous Arbitrage Model. Now, let's consider the continuous-time limit, where arbitrageurs continuously monitor the market and react instantaneously to any arbitrage opportunities. This idealized scenario allows us to capture the dynamics of a highly efficient market with vigilant arbitrageurs.

Formally, we make the following assumption:

Assumption 3.6. Arbitrageurs continuously monitor and immediately act on arbitrage opportunities.

Under this assumption, arbitrageurs continuously adjust their trading strategies to maintain the G3M price within the no-arbitrage bounds. Their actions effectively prevent any significant mispricing from persisting.

The following proposition characterizes the dynamics of the mispricing process in this continuous setting:

Proposition 3.7 (Continuous Mispricing Dynamics). *Given that the market price S_t is continuous and adheres to the initial condition $\gamma P_0 \leq S_0 \leq \gamma^{-1} P_0$, and under Assumptions 3.1, 3.2, and 3.6, we have:*

- a) *The mispricing process, denoted as Z_t , can be decomposed into $Z_t = \ln S_t - \ln P_0 + L_t - U_t$ and takes value within the range $[\ln \gamma, -\ln \gamma]$ for all $t \geq 0$.*
- b) *L_t and U_t are non-decreasing and continuous, with their initial values set at $L_0 = U_0 = 0$.*
- c) *L_t and U_t increase only when $Z_t = -\ln \gamma$ and $Z_t = \ln \gamma$, respectively.*

Furthermore, L_t and U_t satisfy:

$$L_t = \sup_{0 \leq s \leq t} (-\ln(\gamma P_0) + \ln S_s - U_s)^-, \quad (19)$$

$$U_t = \sup_{0 \leq s \leq t} (\ln(\gamma^{-1} P_0) - \ln S_s - L_s)^-. \quad (20)$$

Proof. Following the approach in [FMW24, §3], we decompose the log pool price as $\ln P_t = \ln P_0 + U_t - L_t$, where U_t and L_t represent the cumulative changes in log price due to buy and sell arbitrage orders, respectively. These processes naturally satisfy properties (a) to (c). Equations (19) and (20) then follow directly from the characterization of reflected processes in [Har13, Proposition 2.4]. \square

Remark 3.8. The mispricing process Z_t can be viewed as a stochastic storage system with finite capacity, where L_t and U_t act as reflecting barriers that keep Z_t within the allowed range [Har13, §2.3]. In the special case where the reference market price S_t follows a geometric Brownian motion, Z_t becomes a reflected Brownian motion [Har13, §6].

We now consider the dynamics of the reserve process x_t (or y_t). Time t is a point of increase (or decrease) for x_t if there exists $\delta > 0$ such that $x_{t-\delta_1} < x_{t+\delta_2}$ (or $x_{t-\delta_1} > x_{t+\delta_2}$) for all $\delta_1, \delta_2 \in (0, \delta]$. The reserve process x_t increases (or decreases) only when $Z_t = a$ if, at every point of increase (or decrease) for x_t , $Z_t = a$.

Corollary 3.9 (Inventory Dynamics in Arbitrage). *Under the assumptions of Proposition 3.7, the following hold:*

- (a) *x_t and y_t are predictable processes.*
- (b) *x_t increases only when $Z_t = \ln \gamma$ and decreases only when $Z_t = -\ln \gamma$; y_t increases only when $Z_t = -\ln \gamma$ and decreases only when $Z_t = \ln \gamma$.*
- (c) *$\ln x_t$ and $\ln y_t$ are continuous and of bounded variation on bounded intervals of $[0, \infty)$.*

(d) The arbitrage inventory process can be characterized by

$$\begin{aligned} d \ln x_t &= \frac{1-w}{1-w+\gamma w} dL_t - \frac{\gamma(1-w)}{\gamma(1-w)+w} dU_t, \\ d \ln y_t &= \frac{w}{\gamma(1-w)+w} dU_t - \frac{\gamma w}{1-w+\gamma w} dL_t. \end{aligned} \quad (21)$$

Proof. By Proposition 3.7 (a)–(c), U_t , L_t , and $\ln P_t$ are continuous, predictable processes of bounded variation. The assertions follow directly from (9). \square

The dynamics of liquidity growth based on the mispricing process can be described by incorporating (21) into (10).

Corollary 3.10 (Liquidity Dynamics in Arbitrage). *Under the assumptions of Proposition 3.7, the liquidity process ℓ_t is nondecreasing and predictable. Its rate of change is given by:*

$$d \ln \ell_t = \frac{(1-\gamma)w(1-w)}{1-w+\gamma w} dL_t + \frac{(1-\gamma)w(1-w)}{\gamma(1-w)+w} dU_t. \quad (22)$$

Remark 3.11. The liquidity growth term in (22) corresponds to the excess growth rate (see Section 4.1) in Stochastic Portfolio Theory [Fer02, §1.1] as $\gamma \rightarrow 1$.

3.3. LP Wealth Growth. In this section, we analyze how the wealth of liquidity providers (LPs) evolves in the G3M under arbitrage-driven dynamics. To do this, we express the LP's wealth in terms of the reference market prices and the mispricing process.

The LP's wealth V_t is defined as the total value of their holdings in the pool, denominated in terms of the reference market prices S_t^X and S_t^Y for assets X and Y , respectively. This can be written as:

$$V_t = S_t^X x_t + S_t^Y y_t = S_t^Y (S_t x_t + y_t), \quad (23)$$

where $S_t = S_t^X / S_t^Y$ is the relative price of asset X in the reference market.

Using the relationship between the G3M pool price P_t and the reserves (equation (6)), we can derive bounds on the term $S_t x_t + y_t$:

$$\begin{aligned} S_t x_t + y_t &\geq \gamma P_t x_t + y_t = \gamma (P_t x_t + y_t) + (1-\gamma) y_t = (1-w(1-\gamma)) (P_t x_t + y_t); \\ S_t x_t + y_t &\leq \frac{1}{\gamma} P_t x_t + y_t = \frac{1}{\gamma} (P_t x_t + y_t) + \left(1 - \frac{1}{\gamma}\right) y_t = \left\{1 + w \left(\frac{1}{\gamma} - 1\right)\right\} (P_t x_t + y_t). \end{aligned}$$

These inequalities show that the value of the LP's holdings, $S_t x_t + y_t$, is always within a certain factor of the value based on the G3M pool price, $P_t x_t + y_t$. To quantify this relationship, we define the ratio:

$$d_t := \ln \frac{S_t x_t + y_t}{P_t x_t + y_t}.$$

From the above inequalities, we see that d_t is bounded:

$$1 - w(1-\gamma) \leq d_t \leq 1 + w(\gamma^{-1} - 1).$$

Now, we can express the logarithmic wealth of the LP as:

$$\begin{aligned}\ln V_t &= \ln \ell_t + w \ln S_t^X + (1-w) \ln S_t^Y + d_t - Z_t \\ &= \frac{(1-\gamma)w(1-w)}{1-w+\gamma w} L_t + \frac{(1-\gamma)w(1-w)}{\gamma(1-w)+w} U_t \\ &\quad + w \ln S_t^X + (1-w) \ln S_t^Y + d_t - Z_t,\end{aligned}\tag{24}$$

Note that d_t and Z_t are bounded. This decomposition is the key to understanding the LP wealth growth in the G3M under arbitrage.

4. LP WEALTH GROWTH

This section develops a methodology for calculating the ergodic growth rates of LP wealth components, denoted by L_t , U_t , and V_t . We begin by establishing the stochastic market model that governs the price dynamics of the assets involved.

4.1. Market Model Setup. We consider a market with two assets, X and Y , whose price dynamics are governed by the following SDEs:

$$\begin{aligned}d \ln S_t^X &= \mu_t^X dt + \xi_t^{XX} dB_t^X + \xi_t^{XY} dB_t^Y, \\ d \ln S_t^Y &= \mu_t^Y dt + \xi_t^{YX} dB_t^X + \xi_t^{YY} dB_t^Y,\end{aligned}\tag{25}$$

where μ_t^X , μ_t^Y , ξ_t^{XX} , ξ_t^{XY} , ξ_t^{YX} , and ξ_t^{YY} are measurable and adapted, and B_t^X and B_t^Y are independent Brownian motions. The corresponding covariance processes for $\ln S_t^X$ and $\ln S_t^Y$ are given by

$$\begin{aligned}\sigma_t^{XX} dt &= d\langle \ln S^X, \ln S^X \rangle_t = (\xi_t^{XX} \xi_t^{XX} + \xi_t^{XY} \xi_t^{XY}) dt, \\ \sigma_t^{XY} dt &= d\langle \ln S^X, \ln S^Y \rangle_t = (\xi_t^{XX} \xi_t^{YX} + \xi_t^{XY} \xi_t^{YY}) dt = d\langle \ln S^Y, \ln S^X \rangle_t = \sigma_t^{YX} dt, \\ \sigma_t^{YY} dt &= d\langle \ln S^Y, \ln S^Y \rangle_t = (\xi_t^{YX} \xi_t^{YX} + \xi_t^{YY} \xi_t^{YY}) dt.\end{aligned}\tag{26}$$

In this framework, the AMM price, denoted by P_t , is driven by the relative price of the two assets, $S_t = \frac{S_t^X}{S_t^Y}$. Applying Itô's lemma to S_t , we obtain

$$\begin{aligned}d \ln S_t &= d \ln S_t^X - d \ln S_t^Y \\ &= (\mu_t^X - \mu_t^Y) dt + (\xi_t^{XX} - \xi_t^{YX}) dB_t^X + (\xi_t^{XY} - \xi_t^{YY}) dB_t^Y \\ &:= \mu_t dt + \sigma_t dB_t^{XY},\end{aligned}\tag{27}$$

where $\mu_t = \mu_t^X - \mu_t^Y$, $dB_t^{XY} = \frac{(\sigma_t^{XX})^{\frac{1}{2}}}{\sigma_t} dB_t^X - \frac{(\sigma_t^{YY})^{\frac{1}{2}}}{\sigma_t} dB_t^Y$, and $\sigma_t = \sqrt{\sigma_t^{XX} + \sigma_t^{YY} - 2\sigma_t^{XY}}$.

Finally, we assume the following long-term limits exist:

$$\mu_X := \lim_{T \rightarrow \infty} \frac{\mathbb{E} [\ln S_T^X]}{T}, \quad \mu_Y := \lim_{T \rightarrow \infty} \frac{\mathbb{E} [\ln S_T^Y]}{T}.\tag{28}$$

These limits represent the long-term average growth rates of the asset prices. For convenience, we define $\mu = \mu_X - \mu_Y$, which represents the long-term average growth rate of the relative price S_t .

4.2. Mispricing Process as a Reflected Diffusion. To analyze the dynamics of mispricing, we model the log relative price $s_t := \ln S_t$ as a diffusion process:

$$ds_t = \tilde{\mu}(t, s_t)dt + \tilde{\sigma}(t, s_t)dW_t, \quad (29)$$

where $\tilde{\mu}(t, x)$ and $\tilde{\sigma}(t, x)$ both satisfy the standard Lipschitz and linear growth condition: for any $T > 0$,

$$\sup_{t \in [0, T]} \sup_{x, y \in \mathbb{R}} \left[\frac{|\tilde{\mu}(t, x) - \tilde{\mu}(t, y)| + |\tilde{\sigma}(t, x) - \tilde{\sigma}(t, y)|}{|x - y|} + \frac{|\tilde{\mu}(t, x)| + |\tilde{\sigma}(t, x)|}{1 + |x|} \right] < \infty.$$

Fix a fee tier $\gamma \in (0, 1)$ and set $c = -\ln \gamma$. Suppose that $\ln(S_0/P_0) = z_0 \in (-c, c)$. According to [Har13, Proposition 2.4], s_t uniquely determines a process Z_t that satisfies the following properties:

- Z_t takes values in $[-c, c]$;
- $Z_t = -\ln P_0 + s_t + L_t - U_t$; and
- L_t and U_t are two non-decreasing, continuous processes with $L_0 = U_0 = 0$ that increase only when $Z_t = -c$ and $Z_t = c$, respectively.

Then, by uniqueness, Z_t coincides with the mispricing process in Proposition 3.7. In particular, the mispricing process Z_t evolves according to

$$\begin{cases} dZ_t = ds_t + dL_t - dU_t = \tilde{\mu}(t, s_t)dt + \tilde{\sigma}(t, s_t)dW_t + dL_t - dU_t, \\ Z_0 = z_0 \in [-c, c]. \end{cases} \quad (30)$$

This shows that Z_t is a diffusion process confined to the interval $[-c, c]$. The "reflection" at the boundaries captures the dynamics of mispricing being bounded within a certain range. Throughout, we assume that Z_t follows (30) unless specified otherwise.

One would anticipate that L_t and U_t are boundary local times of Z_t . This is justified by the following lemma. For the basic theory on local times, see [RY99].

Lemma 4.1. *For any $t > 0$,*

$$L_t = \lim_{\varepsilon \rightarrow 0^+} \frac{1}{2\varepsilon} \int_0^t \mathbf{1}_{[-c, -c+\varepsilon)}(Z_r) d\langle Z \rangle_r, \quad (31)$$

$$U_t = \lim_{\varepsilon \rightarrow 0^+} \frac{1}{2\varepsilon} \int_0^t \mathbf{1}_{(c-\varepsilon, c]}(Z_r) d\langle Z \rangle_r, \quad (32)$$

where $d\langle Z \rangle_r = \tilde{\sigma}^2(r, s_r)dr$ and the limits exist in L^2 .

Proof. Let $f_\varepsilon(x)$ be the function such that $f_\varepsilon''(x) = \frac{1}{\varepsilon} \mathbf{1}_{[-c, -c+\varepsilon)}(x)$ and $f_\varepsilon(-c) = f'_\varepsilon(-c) = 0$. By Itô's lemma and the property that L_t and U_t increase only when $Z_t = -c$ and $Z_t = c$ respectively,

$$df_\varepsilon(Z_t) = df'_\varepsilon(Z_t)ds_t + f'_\varepsilon(-c)dL_t - f'_\varepsilon(c)dU_t + \frac{1}{2\varepsilon} \mathbf{1}_{[-c, -c+\varepsilon)}(Z_t) d\langle Z \rangle_t.$$

Since $f'_\varepsilon(-c) = 0$ for all $\varepsilon > 0$ and $f'_\varepsilon(c) = 1$ for small enough ε , it follows that

$$f_\varepsilon(Z_t) - f_\varepsilon(Z_0) = \int_0^t f'_\varepsilon(Z_r)ds_r - U_t + \frac{1}{2\varepsilon} \int_0^t \mathbf{1}_{[-c, -c+\varepsilon)}(Z_r) d\langle Z \rangle_r.$$

As $\varepsilon \rightarrow 0^+$, $f_\varepsilon(x) \rightarrow (x + c)^+$ and $f'_\varepsilon(x) \rightarrow \mathbf{1}_{[-c, \infty)}(x)$. Since $Z_t \in [-c, c]$, we deduce that

$$(Z_t + c) - (Z_0 + c) = \int_0^t 1 ds_r - U_t + \lim_{\varepsilon \rightarrow 0^+} \frac{1}{2\varepsilon} \int_0^t \mathbf{1}_{[-c, -c+\varepsilon]}(Z_r) d\langle Z \rangle_r,$$

where the limit exists in L^2 thanks to Itô's isometry. This and the relation $dZ_t = ds_t + dL_t - dU_t$ from (30) yield (31). Similarly, (32) can be obtained by considering the function $f_\varepsilon(x)$ such that $f''_\varepsilon(x) = \frac{1}{\varepsilon} \mathbf{1}_{(c-\varepsilon, c]}(x)$ and $f_\varepsilon(c) = f'_\varepsilon(c) = 0$. \square

Motivated by the study of the growth rate of LP's wealth, we examine quantities of the form

$$g(Z_T) + \int_t^T f(r, Z_r) dr - \int_t^T \alpha_r dL_r + \int_t^T \beta_r dU_r. \quad (33)$$

The computation of the expectation of (33) simplifies when $\tilde{\mu}$ and $\tilde{\sigma}$ are constant because Z_t has Markov property. However, this is not the case when $\tilde{\mu}$ or $\tilde{\sigma}$ depend on s_t . In order to overcome this technical obstacle, we appeal to the method of mimicking [Kry85, Gyö86] and adapt it to our current setting where local times are involved in the SDE. Define

$$\mu(t, Z_t) = \mathbb{E}[\tilde{\mu}(t, s_t) | Z_t], \quad \sigma(t, Z_t) = \sqrt{\mathbb{E}[\tilde{\sigma}^2(t, s_t) | Z_t]}. \quad (34)$$

Consider the following SDE with reflection:

$$\begin{cases} d\hat{Z}_t = \mu(t, \hat{Z}_t) dt + \sigma(t, \hat{Z}_t) dW_t + d\hat{L}_t - d\hat{U}_t, \\ \hat{Z}_0 = z_0 \in (-c, c), \quad \hat{Z}_t \in [-c, c], \end{cases} \quad (35)$$

where \hat{L}_t and \hat{U}_t are boundary local times of \hat{Z}_t in the sense of Lemma 4.1, i.e.,

$$\hat{L}_t = \lim_{\varepsilon \rightarrow 0^+} \frac{1}{2\varepsilon} \int_0^t \mathbf{1}_{[-c, -c+\varepsilon]}(\hat{Z}_r) d\langle \hat{Z} \rangle_r, \quad (36)$$

$$\hat{U}_t = \lim_{\varepsilon \rightarrow 0^+} \frac{1}{2\varepsilon} \int_0^t \mathbf{1}_{(c-\varepsilon, c]}(\hat{Z}_r) d\langle \hat{Z} \rangle_r. \quad (37)$$

Lemma 4.2. *The SDE (35) has a unique strong solution \hat{Z}_t with continuous sample paths and strong Markov property.*

Proof. By Theorem 3.1 and Remark 3.3 of [LS84], the Skorokhod problem

$$\begin{cases} d\hat{Z}_t = \mu(t, \hat{Z}_t) dt + \sigma(t, \hat{Z}_t) dW_t - dk_t, \\ \hat{Z}_0 = z_0 \in (-c, c), \\ |k|_t = \int_0^t \mathbf{1}_{\{\hat{Z}_r \in \partial[-c, c]\}} d|k|_r, \quad k_t = \int_0^t n(\hat{Z}_r) d|k|_r, \end{cases} \quad (38)$$

where $|k|_t$ denotes the total variation of k_t and $n(x)$ denotes the outward unit normal for $x \in \partial[-c, c]$, has a unique solution (\hat{Z}_t, k_t) where \hat{Z}_t is a $[-c, c]$ -valued continuous process and k_t is a nonnegative continuous bounded variation process. Since $\partial[-c, c] = \{-c, c\}$, $n(-c) = -1$, and $n(c) = 1$, we can write

$$|k|_t = k_t^{-c} + k_t^c \quad \text{and} \quad k_t = k_t^c - k_t^{-c},$$

where k_t^{-c} and k_t^c are two non-decreasing continuous processes with $k_0^{-c} = k_0^c = 0$ that increase only when $\hat{Z}_t = -c$ and $\hat{Z}_t = c$, respectively. In particular,

$$d\hat{Z}_t = \mu(t, \hat{Z}_t)dt + \sigma(t, \hat{Z}_t)dW_t + dk_t^{-c} - dk_t^c.$$

Then, we may use Itô's lemma as in the proof of Lemma 4.1 to show that $k_t^{-c} = \hat{L}_t$ and $k_t^c = \hat{U}_t$, and hence (35) holds. Finally, as we know the solution \hat{Z}_t to (35) is pathwise unique (because if \tilde{Z}_t is another solution, then $(\tilde{Z}_t, \tilde{U}_t - \tilde{L}_t)$ with \tilde{L}_t and \tilde{U}_t being boundary local times of \tilde{Z}_t is a solution to (38) which is known to be unique), it follows from the standard theory that the solution \hat{Z}_t to (35) is weakly unique and hence has strong Markov property; see [Bas98, §I.4–I.5] or [KS91, §5.3–5.4]. \square

In order to avoid technicalities and focus on the main ideas, we impose hereafter the following assumptions:

(1) Strong ellipticity condition:

$$\text{for any } T > 0, \inf_{t \in [0, T]} \inf_{z \in [-c, c]} \sigma^2(t, z) \geq \varepsilon > 0; \quad (39)$$

(2) Existence of marginal densities:

$$\text{for each } t > 0, Z_t \text{ and } \hat{Z}_t \text{ have densities } p(t, z) \text{ and } \hat{p}(t, z), \text{ respectively.} \quad (40)$$

(3) Regularities: μ is C^1 in z , σ is C^2 in z , and $p, \hat{p} \in C^{1,2}((0, T] \times [-c, c])$.

Lemma 4.3 (Mimicking). *For any $t > 0$, the random variables Z_t and \hat{Z}_t share the same marginal distribution.*

Proof. By Itô's lemma, for any test function $f \in C^\infty([-c, c])$,

$$\begin{aligned} & \mathbb{E} \left[f(\hat{Z}_t) \right] - f(z_0) \\ &= \mathbb{E} \left[\int_0^t \left(f_z(\hat{Z}_r) \mu(r, \hat{Z}_r) + \frac{1}{2} f_{zz}(\hat{Z}_r) \sigma^2(r, \hat{Z}_r) \right) dr + \int_0^t f_z(\hat{Z}_r) d\hat{L}_r - \int_0^t f_z(\hat{Z}_r) d\hat{U}_r \right]. \end{aligned} \quad (41)$$

Under (40), it follows that for any smooth test function f vanishing near $\pm c$,

$$\int_{-c}^c f(z) \hat{p}(t, z) dz - f(z_0) = \int_0^t dr \int_{-c}^c dz \left(f_z(z) \mu(r, z) + \frac{1}{2} f_{zz}(z) \sigma^2(r, z) \right) \hat{p}(r, z),$$

where apparently $\hat{p}(t, z)$ denotes the probability density for \hat{Z}_t . Applying ∂_t and integration by parts, we deduce that

$$\int_{-c}^c f(z) \partial_t \hat{p}(t, z) dz = \int_{-c}^c \left(-f(z) \partial_z (\mu(t, z) \hat{p}(t, z)) + \frac{1}{2} f(z) \partial_{zz} (\sigma^2(t, z) \hat{p}(t, z)) \right) dz.$$

This shows that $\hat{p}(t, z)$ solves the Fokker-Planck equation

$$\partial_t \hat{p}(t, z) = -\partial_z (\mu(t, z) \hat{p}(t, z)) + \frac{1}{2} \partial_{zz} (\sigma^2(t, z) \hat{p}(t, z)), \quad t > 0, z \in (-c, c). \quad (42)$$

To derive the boundary conditions for \hat{p} , we first note that for any test function f (but this time not necessarily vanishing at $\pm c$),

$$\begin{aligned}\mathbb{E} \left[\int_0^t f_z(\hat{Z}_r) d\hat{L}_t \right] &= \lim_{\varepsilon \rightarrow 0^+} \frac{1}{2\varepsilon} \mathbb{E} \left[\int_0^t \mathbf{1}_{[-c, -c+\varepsilon)}(\hat{Z}_r) f_z(\hat{Z}_r) \sigma^2(r, \hat{Z}_r) dr \right] \\ &= \lim_{\varepsilon \rightarrow 0^+} \frac{1}{2\varepsilon} \int_0^t \int_{-c}^{-c+\varepsilon} f_z(z) \sigma^2(r, z) \hat{p}(r, z) dz dr \\ &= \frac{1}{2} \int_0^t f_z(-c) \sigma^2(r, -c) \hat{p}(r, -c) dr\end{aligned}$$

and similarly,

$$\mathbb{E} \left[\int_0^t f_z(\hat{Z}_r) d\hat{U}_t \right] = \frac{1}{2} \int_0^t f_z(c) \sigma^2(r, c) \hat{p}(r, c) dr.$$

Then, we may plug these into (41), apply ∂_t , and integrate by parts again to deduce that

$$\begin{aligned}\int_{-c}^c f \partial_t \hat{p} dz &= \int_{-c}^c \left(f_z \mu \hat{p} + \frac{1}{2} f_{zz} \sigma^2 \hat{p} \right) dz - [f_z \sigma^2 p]_{-c}^c \\ &= \int_{-c}^c f \left(-\partial_z(\mu \hat{p}) + \frac{1}{2} \partial_{zz}(\sigma^2 \hat{p}) \right) dz + \left[f \mu \hat{p} - \frac{1}{2} f \partial_z(\sigma^2 \hat{p}) \right]_{-c}^c.\end{aligned}$$

Since \hat{p} satisfies the PDE (42), this implies that \hat{p} satisfies the boundary condition

$$\mu(t, z) \hat{p}(t, z) - \frac{1}{2} \partial_z(\sigma^2(t, z) \hat{p}(t, z)) = 0 \quad \text{at } z = \pm c. \quad (43)$$

On the other hand, we may apply Itô's lemma to $f(Z_t)$ and use Fubini's theorem and the tower property to show that

$$\begin{aligned}\mathbb{E}[f(Z_t)] - f(z_0) &= \mathbb{E} \left[\int_0^t \left(f_z(Z_r) \tilde{\mu}(r, s_r) + \frac{1}{2} f_{zz}(Z_r) \tilde{\sigma}^2(r, s_r) \right) dr + \int_0^t f_z(Z_r) dL_r - \int_0^t f_z(Z_r) dU_r \right] \\ &= \mathbb{E} \left[\int_0^t \left(f_z(Z_r) \mathbb{E}[\tilde{\mu}(r, s_r) | Z_r] + \frac{1}{2} f_{zz}(Z_r) \mathbb{E}[\tilde{\sigma}^2(r, s_r) | Z_r] \right) dr + \int_0^t f_z(Z_r) dL_r - \int_0^t f_z(Z_r) dU_r \right] \\ &= \mathbb{E} \left[\int_0^t \left(f_z(Z_r) \mu(r, Z_r) + \frac{1}{2} f_{zz}(Z_r) \sigma^2(r, Z_r) \right) dr + \int_0^t f_z(Z_r) dL_r - \int_0^t f_z(Z_r) dU_r \right].\end{aligned}$$

With this, we repeat the same calculations above and deduce that $p(t, z)$ also solves the same PDE (42) with the same boundary condition (43) and the same initial condition δ_{z_0} . Strong ellipticity (39) ensures uniqueness of the solution (see Appendix A), and hence $p(t, z) = \hat{p}(t, z)$ for all $t > 0$ and $z \in [-c, c]$. This completes the proof that Z_t and \hat{Z}_t share the same marginal distribution. \square

Even though the law of the mimicking process \hat{Z} may not be the same as Z (particularly when $\tilde{\mu}$ and $\tilde{\sigma}$ are non-constant), the next lemma shows that the computation of the expectation in (33) may be reduced to the computation of the same quantity for the mimicking process \hat{Z}_t .

Lemma 4.4. *For any given deterministic functions α_t and β_t of t , the following equality holds.*

$$\begin{aligned} & \mathbb{E} \left[g(Z_T) + \int_t^T f(r, Z_r) dr - \int_t^T \alpha_r dL_r + \int_t^T \beta_r dU_r \right] \\ &= \mathbb{E} \left[g(\hat{Z}_T) + \int_t^T f(r, \hat{Z}_r) dr - \int_t^T \alpha_r d\hat{L}_r + \int_t^T \beta_r d\hat{U}_r \right]. \end{aligned} \quad (44)$$

Proof. According to Lemma 4.3, Z_t and \hat{Z}_t have the same marginal distribution, it follows that $\mathbb{E}[g(Z_T)] = \mathbb{E}[g(\hat{Z}_T)]$ and

$$\mathbb{E} \left[\int_t^T f(r, Z_r) dr \right] = \int_t^T \mathbb{E}[f(r, Z_r)] dr = \int_t^T \mathbb{E}[f(r, \hat{Z}_r)] dr = \mathbb{E} \left[\int_t^T f(r, \hat{Z}_r) dr \right]$$

by applying Fubini's theorem. Moreover, thanks to Lemma 4.1 and the tower property,

$$\begin{aligned} \mathbb{E} \left[\int_t^T \alpha_r dL_r \right] &= \lim_{\varepsilon \rightarrow 0^+} \frac{1}{2\varepsilon} \int_t^T \alpha_r \mathbb{E} [\mathbf{1}_{[-c, -c+\varepsilon)}(Z_r) \tilde{\sigma}^2(r, s_r)] dr \\ &= \lim_{\varepsilon \rightarrow 0^+} \frac{1}{2\varepsilon} \int_t^T \alpha_r \mathbb{E} [\mathbf{1}_{[-c, -c+\varepsilon)}(Z_r) \mathbb{E} [\tilde{\sigma}^2(r, s_r) | Z_r]] dr \\ &= \lim_{\varepsilon \rightarrow 0^+} \frac{1}{2\varepsilon} \int_t^T \alpha_r \mathbb{E} [\mathbf{1}_{[-c, -c+\varepsilon)}(Z_r) \sigma^2(r, Z_r)] dr \\ &= \mathbb{E} \left[\int_t^T \alpha_r d\hat{L}_r \right], \end{aligned}$$

where we have used (36) in the last equality. The same applies to the integral for dU_t . This concludes the proof. \square

The following lemma yields a Feynman-Kac type formula, which provides a useful tool for analyzing the conditional expectation in (46) through the PDE (45).

Lemma 4.5. *For any given deterministic functions α_t and β_t of t , the solution $u(t, z)$ to the following parabolic PDE*

$$u_t + \frac{\sigma^2(t, z)}{2} u_{zz} + \mu(t, z) u_z + f(t, z) = 0 \quad (45)$$

with boundary condition

$$u_z(t, -c) = \alpha_t, \quad u_z(t, c) = \beta_t$$

and terminal condition $u(T, z) = g(z)$ has the following stochastic representation

$$u(t, z) = \mathbb{E} \left[g(\hat{Z}_T) + \int_t^T f(r, \hat{Z}_r) dr - \int_t^T \alpha_r d\hat{L}_r + \int_t^T \beta_r d\hat{U}_r \middle| \hat{Z}_t = z \right], \quad (46)$$

where \hat{Z}_t is the reflected diffusion given by (35).

Proof. Itô's lemma implies that

$$u(T, \hat{Z}_T) - u(t, \hat{Z}_t) = \int_t^T \left(u_t + \mu(r, \hat{Z}_r)u_z + \frac{1}{2}\sigma^2(r, \hat{Z}_r)u_{zz} \right) dr + \int_t^T \sigma(r, \hat{Z}_r)u_z dW_r + \int_t^T u_z d\hat{L}_r - \int_t^T u_z d\hat{U}_r,$$

where u_t , u_z and u_{zz} are shorthands for $u_t(r, \hat{Z}_r)$, $u_z(r, \hat{Z}_r)$ and $u_{zz}(r, \hat{Z}_r)$, respectively. Next, we take conditional expectation with respect to the filtration $\hat{\mathcal{F}}_t$ of \hat{Z}_t on both sides of the last equation. Using the boundary and terminal conditions of u and the martingale property of $\int_0^t \sigma(r, \hat{Z}_r)u_z dW_r$, we deduce that

$$\begin{aligned} & \mathbb{E} \left[g(\hat{Z}_T) \mid \hat{\mathcal{F}}_t \right] - u(t, \hat{Z}_t) \\ &= \mathbb{E} \left[\int_t^T \left(u_t + \mu(r, \hat{Z}_r)u_z + \frac{1}{2}\sigma^2(r, \hat{Z}_r)u_{zz} \right) dr + \int_t^T u_z d\hat{L}_r - \int_t^T u_z d\hat{U}_r \mid \hat{\mathcal{F}}_t \right] \\ &= \mathbb{E} \left[- \int_t^T f(r, \hat{Z}_r) dr + \int_t^T \alpha_r d\hat{L}_r - \int_t^T \beta_r d\hat{U}_r \mid \hat{\mathcal{F}}_t \right] \end{aligned}$$

since u satisfies the PDE (45). Thanks to the Markov property of \hat{Z}_t , we may replace $\hat{\mathcal{F}}_t$ by \hat{Z}_t and rearrange terms to obtain the stochastic representation (46). \square

In general, the solution to the terminal-boundary value problem in Lemma 4.5 admits no simple analytical expression. We will focus on two special cases where the eigensystem associated with the operator in (47) is readily accessible. To handle these cases, we introduce the following lemma, which addresses parabolic PDEs with non-zero Neumann boundary conditions.

Lemma 4.6. *The solution u to the parabolic PDE*

$$u_t + \frac{\sigma^2(t, x)}{2}u_{xx} + \mu(t, x)u_x = 0 \quad (47)$$

with boundary conditions $u_x(t, -c) = a$, $u_x(t, c) = b$ for some constants a , b , and terminal condition $u(T, x) = 0$ is given by

$$u(t, x) = v(t, x) + \frac{b-a}{4c}x^2 + \frac{b+a}{2}x, \quad (48)$$

where v is the solution to the following inhomogeneous parabolic PDE

$$v_t + \frac{\sigma^2(t, x)}{2}v_{xx} + \mu(t, x)v_x + \frac{\sigma^2(x)}{2}\frac{b-a}{2c} + \mu(x) \left(\frac{b-a}{2c}x + \frac{b+a}{2} \right) = 0$$

with Neumann boundary conditions $v_x(t, -c) = v_x(t, c) = 0$ and terminal condition

$$v(T, x) = -\frac{b-a}{4c}x^2 - \frac{b+a}{2}x.$$

Proof. The result follows from straightforward calculations. \square

4.3. Time-homogeneous reflected diffusion. This section focuses on the scenario where the reflected diffusion \hat{Z}_t defined by (35) is time-homogeneous. This means that the conditional drift μ and volatility σ in (34) are independent of time. In this case, we can leverage the eigensystem of the infinitesimal generator of \hat{Z}_t to simplify the analysis and express the conditional expectation in (46).

In the time-homogeneous case, the infinitesimal generator is $\mathcal{L} = \frac{1}{2}\sigma^2(x)\partial_x^2 + \mu(x)\partial_x$ with Neumann boundary condition. In the Sturm-Liouville form (see (60)),

$$\mathcal{L} = \frac{1}{\omega(x)} \frac{\partial}{\partial x} \left(p(x) \frac{\partial}{\partial x} \right),$$

where

$$p(x) := e^{\int \frac{2\mu(x)}{\sigma^2(x)} dx}, \quad \omega(x) := \frac{2}{\sigma^2(x)} e^{\int \frac{2\mu(x)}{\sigma^2(x)} dx}.$$

Here, ω represents the **speed measure** from classical diffusion theory, which measures how quickly the diffusion moves through different regions of the state space.

Let $\{(\lambda_n, e_n(x))\}_{n=0}^\infty$ be the normalized eigensystem associated with \mathcal{L} with Neumann boundary condition in the interval $[-c, c]$. This eigensystem provides a convenient basis for analysis. The following theorem presents an eigensystem expansion for conditional expectations of integrals with respect to the boundary local times.

Theorem 4.7. *For a time-homogeneous reflected diffusion \hat{Z}_t defined by (35) and any constants a and b , the conditional expectation*

$$\mathbb{E} \left[- \int_t^T ad\hat{L}_\tau + \int_t^T bd\hat{U}_\tau \mid \hat{Z}_t = x \right] \quad (49)$$

admits the following eigensystem expansion associated with \mathcal{L} with Neumann boundary condition:

$$\begin{aligned} & \mathbb{E} \left[- \int_t^T ad\hat{L}_\tau + \int_t^T bd\hat{U}_\tau \mid \hat{Z}_t = x \right] \\ &= \frac{b-a}{4c}x^2 + \frac{b+a}{2}x + \xi_0(T-t) - \eta_0 + \sum_{n=1}^{\infty} \left\{ \frac{\xi_n}{\lambda_n} [1 - e^{-\lambda_n(T-t)}] - \eta_n e^{-\lambda_n(T-t)} \right\} e_n(x), \end{aligned} \quad (50)$$

where the coefficients ξ_n and η_n , for $n \geq 0$, are given by

$$\xi_n = \int_{-c}^c h(x)e_n(x)\omega(x)dx, \quad \eta_n = \int_{-c}^c k(x)e_n(x)\omega(x)dx \quad (51)$$

with

$$h(x) = \frac{\sigma^2(x)}{2} \frac{b-a}{2c} + \mu(x) \left(\frac{b-a}{2c}x + \frac{b+a}{2} \right), \quad k(x) = -\frac{b-a}{4c}x^2 - \frac{b+a}{2}x.$$

Proof. Let $u(t, z)$ denote the conditional expectation in (49). Then, by Lemma 4.5, u satisfies the PDE

$$u_t + \frac{\sigma^2(x)}{2}u_{xx} + \mu(x)u_x = 0$$

with boundary condition $u_x(t, -c) = a$, $u_x(t, c) = b$, for all $t < T$, and terminal condition $u(T, x) = 0$. Thus, by Lemma 4.6, the solution u can be written as

$$u(t, x) = v(t, x) + \frac{b-a}{4c}x^2 + \frac{b+a}{2}x,$$

where v is the solution to the following inhomogeneous parabolic PDE

$$v_t + \frac{\sigma^2(x)}{2}v_{xx} + \mu(x)v_x + \frac{\sigma^2(x)}{2}\frac{b-a}{2c} + \mu(x)\left(\frac{b-a}{2c}x + \frac{b+a}{2}\right) = 0$$

with Neumann boundary conditions $v_x(t, -c) = v_x(t, c) = 0$ and terminal condition

$$v(T, x) = -\frac{b-a}{4c}x^2 - \frac{b+a}{2}x.$$

Hence, the eigensystem expansion for v as in (50) in Section B is given by

$$v(t, x) = \xi_0(T-t) - \eta_0 + \sum_{n=1}^{\infty} \left\{ \frac{\xi_n}{\lambda_n} \left[1 - e^{-\lambda_n(T-t)} \right] - \eta_n e^{-\lambda_n(T-t)} \right\} e_n(x),$$

where the coefficients ξ_n 's and η_n 's are defined in (51). Finally, since

$$\mathbb{E} \left[- \int_t^T a d\hat{L}_\tau + \int_t^T b d\hat{U}_\tau \mid \hat{Z}_t = x \right] = u(t, x) = \frac{b-a}{4c}x^2 + \frac{b+a}{2}x + v(t, x),$$

it follows that the eigensystem expansion (50) holds. \square

This theorem provides a concrete way to calculate the conditional expectation in (49) using the eigensystem of \mathcal{L} . This result enables us to analyze the long-term behavior of the mispricing process and its impact on LP's wealth.

Corollary 4.8. *As $T \rightarrow \infty$, the limit of time-average of the expectation of (49) is given by*

$$\begin{aligned} & \lim_{T \rightarrow \infty} \frac{1}{T-t} \mathbb{E} [-a(L_T - L_t) + b(U_T - U_t)] \\ &= \xi_0 = \frac{\int_{-c}^c \left\{ \frac{\sigma^2(x)}{2} \frac{b-a}{2c} + \mu(x) \left(\frac{b-a}{2c}x + \frac{a+b}{2} \right) \right\} \omega(x) dx}{\int_{-c}^c \omega(x) dx}. \end{aligned}$$

Proof. Thanks to (50), we have

$$\lim_{T \rightarrow \infty} \frac{1}{T-t} \mathbb{E} \left[-a(\hat{L}_T - \hat{L}_t) + b(\hat{U}_T - \hat{U}_t) \mid \hat{Z}_t \right] = \xi_0 \quad \text{a.s.}$$

We may apply expectation to the above and apply dominated convergence theorem to pass the limit under expectation, and then use Lemma 4.4 to finish the proof. \square

This corollary, which can also be found in [GW13], provides a concise expression for the long-term average behavior of the processes L_t and U_t , which regulate the reflection of the mispricing process at the boundaries.

Leveraging this result, we can determine the long-term expected logarithmic growth rate of an LP's wealth in the G3M model.

Theorem 4.9 (Log Growth Rate of LP Wealth in G3M Time-homogeneous). *Assuming that the functions μ and σ defined in (34) are independent of t , the long-term expected logarithmic growth rate of an LP's wealth in a G3M is given by*

$$\lim_{T \rightarrow \infty} \frac{\mathbb{E}[\ln V_T]}{T} = w\mu_X + (1-w)\mu_Y + \frac{(1-\gamma)w(1-w)}{1-w+\gamma w}\alpha + \frac{(1-\gamma)w(1-w)}{\gamma(1-w)+w}\beta, \quad (52)$$

where μ_X and μ_Y are the long-term growth rates of the asset prices defined in (28), and

$$\begin{aligned} \alpha &= \frac{\int_{\ln \gamma}^{-\ln \gamma} - \left\{ \frac{\sigma^2(x)}{4 \ln \gamma} + \mu(x) \left(\frac{1}{2 \ln \gamma} x - \frac{1}{2} \right) \right\} \omega(x) dx}{\int_{\ln \gamma}^{-\ln \gamma} \omega(x) dx}, \\ \beta &= \frac{\int_{\ln \gamma}^{-\ln \gamma} - \left\{ \frac{\sigma^2(x)}{4 \ln \gamma} + \mu(x) \left(\frac{1}{2 \ln \gamma} x + \frac{1}{2} \right) \right\} \omega(x) dx}{\int_{\ln \gamma}^{-\ln \gamma} \omega(x) dx}, \\ \omega(x) &= \frac{2}{\sigma^2(x)} e^{\int \frac{2\mu(x)}{\sigma^2(x)} dx}. \end{aligned}$$

Proof. This result follows directly from combining the expression for the logarithmic growth rate of LP's wealth (24), the definitions of μ_X and μ_Y (28), and Corollary 4.8. \square

Theorem 4.9 provides a practical method for calculating the long-term growth rate of an LP's wealth. The terms α and β quantify the influence of mispricing on this growth rate, capturing the effects of the boundaries on mispricing and the speed measure.

Remark 4.10. Theorem 4.9 reveals an intriguing connection between liquidity wealth dynamics in G3Ms under arbitrage-driven scenarios and the principles of Stochastic Portfolio Theory (SPT), particularly in frictionless markets. More precisely, Equation (52) corresponds to the growth rate

$$w\mu_X + (1-w)\mu_Y + \frac{w(1-w)}{2}\sigma^2$$

of a constant rebalanced portfolio with the same weight, as discussed in [Fer02, §1.1]. Furthermore, the term $\frac{(1-\gamma)w(1-w)}{1-w+\gamma w}\alpha + \frac{(1-\gamma)w(1-w)}{\gamma(1-w)+w}\beta$ converges to the excess growth rate $\frac{w(1-w)}{2}\sigma^2$ as the fee tier γ approaches 1.

4.4. Optimal fees and optimal growth. To illustrate the link between LP wealth growth and SPT (as discussed in Remark 4.10), we consider a G3M operating within a GBM market model. This simplifies the market dynamics in (25) by assuming constant parameters for the asset prices. Consequently, the covariance processes in (26) also have constant parameters, and the relative price $S_t = S_t^X/S_t^Y$ follows a simpler SDE:

$$d \ln S_t = \mu dt + \sigma dB_t,$$

where μ and σ are constants defined in (27). This simplified setting allows us to explicitly compute the long-term expected logarithmic growth rate of LP wealth using Theorem 4.9.

Corollary 4.11 (Log Growth Rate of LP under GBM). *In a G3M operating under a GBM market with constant drift μ and volatility σ , the long-term logarithmic growth rate of LP*

wealth is:

$$\lim_{T \rightarrow \infty} \frac{\mathbb{E}[\ln V_T]}{T} = w\mu_X + (1-w)\mu_Y + \frac{(1-\gamma)w(1-w)}{1-w+\gamma w}\alpha + \frac{(1-\gamma)w(1-w)}{\gamma(1-w)+w}\beta,$$

where $\theta = \frac{2\mu}{\sigma^2}$ and

- $\alpha = \beta = -\frac{\sigma^2}{4\ln\gamma}$ if $\theta = 0$.
- $\alpha = \frac{\theta\sigma^2}{2(\gamma^{-2\theta}-1)}$ and $\beta = \frac{\theta\sigma^2}{2(1-\gamma^{2\theta})}$ if $\theta \neq 0$.

Furthermore, the steady-state distribution π of the mispricing process Z_t is:

- If $\theta = 0$, then π is the uniform distribution on $[\ln\gamma, -\ln\gamma]$.
- If $\theta \neq 0$, π is the truncated exponential distribution

$$\pi(dz) = \frac{\theta e^{\theta z}}{\gamma^{-\theta} - \gamma^\theta} dz, \quad z \in [\ln\gamma, -\ln\gamma].$$

Proof. Under the GBM assumption, the conditional expectations in (34) are constants and coincide with μ and σ . In particular,

$$\begin{aligned} \omega(x) &= \begin{cases} \frac{2}{\sigma^2} & \text{if } \theta = 0, \\ \frac{2}{\sigma^2} e^{\theta x} & \text{if } \theta \neq 0, \end{cases} \\ \int_{\ln\gamma}^{-\ln\gamma} \omega(x) dx &= \begin{cases} \frac{-2\ln\gamma}{\sigma^2} & \text{if } \theta = 0, \\ \frac{1}{\mu} [\gamma^{-\theta} - \gamma^\theta] & \text{if } \theta \neq 0, \end{cases} \\ \int_{\ln\gamma}^{-\ln\gamma} x\omega(x) dx &= \begin{cases} 0 & \text{if } \theta = 0, \\ \frac{-\ln\gamma}{\mu} [\gamma^{-\theta} + \gamma^\theta] + \frac{1}{\theta\mu} [\gamma^{-\theta} - \gamma^\theta] & \text{if } \theta \neq 0. \end{cases} \end{aligned}$$

Hence, the first part of the corollary follows directly from Theorem 4.9. Furthermore, since μ and σ are constant, the mispricing process Z_t coincides with the reflected diffusion \hat{Z}_t defined by (35). Therefore, the second part of the corollary follows from Theorem B.2 in the appendix. \square

Remark 4.12. This result is consistent with the calculation in [Har13, Proposition 6.6], which utilizes the stationary distribution of the mispricing process.

4.4.1. Numerical Analysis and Optimal Fees. We now numerically investigate the growth rate of LP wealth in G3Ms across different fee tiers γ and asset weights w . This analysis extends the work in [TW20, §5], which focused on the specific case of $w = \frac{1}{2}$.

To quantify the impact of fees, we define $g(w, \gamma)$ as the ratio of the "mispricing-related" term in the G3M growth rate to the excess return in SPT. Corollary 4.11 yields

$$g(w, \gamma) = \begin{cases} -\frac{1}{2\ln\gamma} \left\{ \frac{1-\gamma}{1-w+\gamma w} + \frac{1-\gamma}{\gamma(1-w)+w} \right\} & \text{if } \theta = 0; \\ \theta \left\{ \frac{1-\gamma}{1-w+\gamma w} \frac{\gamma^{2\theta}}{1-\gamma^{2\theta}} + \frac{1-\gamma}{\gamma(1-w)+w} \frac{1}{1-\gamma^{2\theta}} \right\} & \text{if } \theta \neq 0. \end{cases}$$

Figures 2 and 3 illustrate this growth rate ratio for various weights and values of $\theta = \frac{2\mu}{\sigma^2}$. These figures reveal interesting "phase transitions" for both θ and w , where the ratio can exhibit non-monotonicity. This suggests that the optimal fee tier γ^* that maximizes LP

wealth growth may lie within the interior of the interval $(0, 1)$, a behavior not observed when $w = \frac{1}{2}$.

The figures also highlight the symmetry of $g(w, \gamma)$ with respect to θ and $w = \frac{1}{2}$.

- By replacing θ with $-\theta$, we obtain

$$\begin{aligned} & -\theta(1-\gamma) \left\{ \frac{1}{1-w+\gamma w} \frac{\gamma^{-2\theta}}{1-\gamma^{-2\theta}} + \frac{1}{\gamma(1-w)+w} \frac{1}{1-\gamma^{-2\theta}} \right\} \\ &= -\theta(1-\gamma) \left\{ \frac{1}{1-w+\gamma w} \frac{1}{\gamma^{2\theta}-1} + \frac{1}{\gamma(1-w)+w} \frac{\gamma^{2\theta}}{\gamma^{2\theta}-1} \right\} \\ &= \theta(1-\gamma) \left\{ \frac{1}{1-w+\gamma w} \frac{1}{1-\gamma^{2\theta}} + \frac{1}{\gamma(1-w)+w} \frac{\gamma^{2\theta}}{1-\gamma^{2\theta}} \right\}, \end{aligned}$$

which explains the symmetry between the plots for positive and negative values of θ in Figure 2.

- Let $\delta = w - \frac{1}{2}$. Then, g can be expressed in terms of δ as

$$g(\delta, \gamma) = \begin{cases} -\frac{1}{2\ln\gamma} \left\{ \frac{1-\gamma}{\frac{1}{2}(1+\gamma)+(\gamma-1)\delta} + \frac{1-\gamma}{\frac{1}{2}(1+\gamma)-(\gamma-1)\delta} \right\} & \text{if } \theta = 0; \\ \theta \left\{ \frac{1-\gamma}{\frac{1}{2}(1+\gamma)+(\gamma-1)\delta} \frac{\gamma^{2\theta}}{1-\gamma^{2\theta}} + \frac{1-\gamma}{\frac{1}{2}(1+\gamma)-(\gamma-1)\delta} \frac{1}{1-\gamma^{2\theta}} \right\} & \text{if } \theta \neq 0. \end{cases}$$

For $\theta = 0$, we have $g(-\delta, \gamma) = g(\delta, \gamma)$, explaining why only "red colors" appear when $\theta = 0$ in Figures 2 and 3. For $\theta \neq 0$, a similar symmetry around $\delta = 0$ (i.e., $w = \frac{1}{2}$) is observed, as shown in Figure 2.

Heatmaps in Figures 4 and 5 further visualize the growth rate ratio. The location of the maximum value in each row is labeled, emphasizing the potential for non-monotonicity and interior optimal fee tiers. Notably, under certain conditions, the G3M can outperform both the unrebalanced ($\gamma^* = 0$) and constant rebalanced ($\gamma^* = 1$) portfolio strategies.

4.5. Time-inhomogeneous reflected diffusion. In Section 4.3, we utilized the eigensystem of the infinitesimal generator to analyze the long-term growth rate of LP wealth for the time-homogeneous case. However, this approach is not applicable when the drift and volatility coefficients are time-dependent, as there are no universal eigenfunctions associated with time-varying eigenvalues.

Nevertheless, we can still determine the long-term expected logarithmic growth rate by analyzing the asymptotic behavior of the time-averaged expectation. This section presents a method to achieve this for time-inhomogeneous reflected diffusions.

Recall the mispricing process Z_t governed by (30):

$$dZ_t = \tilde{\sigma}(t, s_t) dW_t + \tilde{\mu}(t, s_t) dt + dL_t - dU_t.$$

We assume that the time-dependent drift $\mu(t, z)$ and volatility $\sigma(t, z)$ defined in (34) converge to limiting functions as $t \rightarrow \infty$:

$$\lim_{t \rightarrow \infty} \sigma(t, z) = \sigma(z), \quad \lim_{t \rightarrow \infty} \mu(t, z) = \mu(z)$$

in the L^2 sense, and that these limits are smooth and bounded. This implies that the mispricing process eventually approaches a time-homogeneous behavior. Define the limiting

speed measure $q(y)$ as:

$$q(y) = \frac{w(y)}{\int_{-c}^c w(\eta) d\eta}, \quad \text{where } w(y) := \frac{2}{\sigma^2(y)} e^{\int \frac{2\mu(y)}{\sigma^2(y)} dy}.$$

This speed measure corresponds to the stationary distribution of the limiting time-homogeneous reflected diffusion with drift $\mu(x)$ and volatility $\sigma(x)$.

The following theorem, whose proof is deferred to Appendix C, characterizes the long-term time-averaged expectation for time-inhomogeneous reflected diffusions.

Theorem 4.13. *Let $u = u(t, x)$ be the solution to the parabolic PDE*

$$u_t + \frac{\sigma^2(t, x)}{2} u_{xx} + \mu(t, x) u_x + f(t, x) = 0$$

with Neumann boundary condition $u_x(t, -c) = u_x(t, c) = 0$ and terminal condition $u(T, x) = g(x)$. Assume that $g \in L^2$ and there exists a function $\bar{f}(x)$ such that

$$\lim_{t \rightarrow \infty} f(t, x) = \bar{f}(x)$$

in L^2 . Then, the following asymptotic behavior holds for $u(t, x)$ as $T \rightarrow \infty$:

$$\lim_{T \rightarrow \infty} \frac{u(t, x)}{T - t} = \int_{-c}^c \bar{f}(y) q(y) dy.$$

This theorem provides a tool for analyzing the long-term behavior of time-inhomogeneous reflected diffusions. As a direct consequence, we obtain the following result for the long-term growth rate of LP wealth in the G3M model.

Corollary 4.14 (Log Growth Rate of LP Wealth in G3M Time-inhomogeneous). *Assume that the mispricing process Z_t is governed by (30) with time-dependent coefficients $\sigma(t, z)$ and $\mu(t, z)$ defined in (34) converging to smooth and bounded limits $\sigma(z)$ and $\mu(z)$ in the L^2 sense as $t \rightarrow \infty$. Then, the long-term expected logarithmic growth rate of LP wealth in a G3M is:*

$$\lim_{T \rightarrow \infty} \frac{\mathbb{E}[\ln V_T]}{T} = w\mu_X + (1-w)\mu_Y + \frac{(1-\gamma)w(1-w)}{1-w+\gamma w} \alpha + \frac{(1-\gamma)w(1-w)}{\gamma(1-w)+w} \beta,$$

where

$$\begin{aligned} \alpha &= \frac{\int_{\ln \gamma}^{-\ln \gamma} - \left\{ \frac{\sigma^2(x)}{4 \ln \gamma} + \mu(x) \left(\frac{1}{2 \ln \gamma} x - \frac{1}{2} \right) \right\} \bar{\omega}(x) dx}{\int_{\ln \gamma}^{-\ln \gamma} \omega(x) dx}, \\ \beta &= \frac{\int_{\ln \gamma}^{-\ln \gamma} - \left\{ \frac{\sigma^2(x)}{4 \ln \gamma} + \mu(x) \left(\frac{1}{2 \ln \gamma} x + \frac{1}{2} \right) \right\} \omega(x) dx}{\int_{\ln \gamma}^{-\ln \gamma} \omega(x) dx}, \\ \omega(x) &= \frac{2}{\sigma^2(x)} e^{\int \frac{2\mu(x)}{\sigma^2(x)} dx}. \end{aligned}$$

This corollary generalizes Theorem 4.9 to the time-inhomogeneous case, demonstrating that the long-term growth rate of LP wealth can be expressed in a similar form, with the limiting speed measure $q(y)$ playing a key role.

4.6. Independent stochastic volatility and drift. In this section, we generalize the analysis to incorporate stochastic volatility and drift in the log price process, $s_t = \ln S_t$. Specifically, we assume s_t follows the diffusion process:

$$ds_t = \tilde{\mu}_t dt + \tilde{\sigma}_t dW_t,$$

where both $\tilde{\mu}_t$ and $\tilde{\sigma}_t$ are stochastic processes but are independent of the driving Brownian motion W_t . This allows for more realistic modeling of market dynamics where volatility and expected returns can fluctuate randomly over time. The mispricing process, $Z_t = \ln S_t - \ln P_t$, remains a reflected diffusion within the interval $[-c, c]$, where $c = -\ln \gamma$, and satisfies

$$dZ_t = ds_t + dL_t - dU_t = \tilde{\mu}_t dt + \tilde{\sigma}_t dW_t + dL_t - dU_t.$$

We further impose a strong ellipticity condition on the volatility, requiring $\tilde{\sigma}_t \geq \epsilon > 0$ almost surely for all t . This ensures that the volatility remains strictly positive.

Our goal is to derive the long-term limit of the time-averaged logarithmic growth rate of LP wealth in this setting. As in Section 4.5, the eigensystem approach used in Section 4.3 is not applicable here because the time-dependent drift $\tilde{\mu}_t \neq 0$ prevents the existence of time-independent eigenfunctions.

4.6.1. Time-Dependent Volatility. To begin, we consider a simplified scenario where the volatility $\tilde{\sigma}_t$ is a deterministic function of t and the drift is zero ($\tilde{\mu}_t = 0$ for all t). This allows us to isolate the effect of time-dependent volatility. In this case, the infinitesimal generator becomes time-dependent:

$$\mathcal{L}_t = \frac{\sigma^2(t)}{2} \partial_x^2.$$

Despite the time-dependence, we can still find eigenvalues and eigenfunctions associated with \mathcal{L}_t that satisfy the eigenvalue problem:

$$\mathcal{L}_t u = \frac{\sigma^2(t)}{2} u_{xx} = -\lambda u$$

with Neumann boundary conditions $u_x(-c) = u_x(c) = 0$. The solutions are:

$$\lambda_n(t) = \frac{\sigma^2(t)}{2} \left(\frac{n\pi}{c} \right)^2, \quad e_0(x) = \sqrt{\frac{1}{2c}}, \quad e_n(x) = \sqrt{\frac{1}{c}} \cos \left(\frac{n\pi}{c} x \right) \text{ for } n \geq 1. \quad (53)$$

Importantly, while the eigenvalues λ_n are time-dependent, the eigenfunctions e_n are not.

Using a similar approach as in Section 4.3, we can express the conditional expectation

$$\mathbb{E}[-a(\hat{L}_T - \hat{L}_t) + b(\hat{U}_T - \hat{U}_t) \mid \hat{Z}_t = x]$$

in terms of the eigensystem (53). This leads to the following theorem (presented without proof):

Theorem 4.15. *Let \hat{Z}_t be the reflected diffusion defined by (35) where $\mu = 0$ and σ is a deterministic function of t . Then, for given constants a and b , the conditional expectation*

$$\mathbb{E} \left[- \int_t^T a d\hat{L}_\tau + \int_t^T b d\hat{U}_\tau \mid \hat{Z}_t = x \right] \quad (54)$$

can be written in terms of the eigensystem (53) associated with \mathcal{L}_t with Neumann boundary condition as

$$\mathbb{E} \left[- \int_t^T ad\hat{L}_\tau + \int_t^T bd\hat{U}_\tau \mid \hat{Z}_t = x \right] = \frac{b-a}{4c}x^2 + \frac{b+a}{2}x + \sum_{n=0}^{\infty} v_n(t)e_n(x), \quad (55)$$

where the time-dependent coefficients v_n are given by

$$v_n(t) = e^{-\frac{1}{2} \left(\frac{n\pi}{c} \right)^2 \int_t^T \sigma^2(s)ds} k_n + \int_t^T h_n(s) e^{-\frac{1}{2} \left(\frac{n\pi}{c} \right)^2 \int_t^s \sigma^2(\tau)d\tau} ds. \quad (56)$$

and

$$h_n(t) = \frac{\sigma^2(t)}{4c} \int_{-c}^c (b-a)e_n(x)dx, \quad k_n = - \int_{-c}^c \left(\frac{b-a}{4c}x^2 + \frac{b+a}{2}x \right) e_n(x)dx.$$

Observe from (55) that we have

$$\begin{aligned} \lim_{T \rightarrow \infty} \frac{1}{T-t} v_n(t) &= 0 \quad \forall n \geq 1, \\ \lim_{T \rightarrow \infty} \frac{1}{T-t} v_0(t) &= \lim_{T \rightarrow \infty} \frac{1}{T-t} k_0 + \lim_{T \rightarrow \infty} \frac{1}{T-t} \int_t^T h_0(s)ds \\ &= \frac{b-a}{4c} \sqrt{2c} \lim_{T \rightarrow \infty} \frac{1}{T-t} \int_t^T \sigma^2(s)ds. \end{aligned}$$

Consequently,

$$\begin{aligned} &\lim_{T \rightarrow \infty} \frac{1}{T-t} \mathbb{E} \left[-a(\hat{L}_T - \hat{L}_t) + b(\hat{U}_T - \hat{U}_t) \mid \hat{Z}_t \right] \\ &= \lim_{T \rightarrow \infty} \frac{1}{T-t} \left\{ \sum_{n=0}^{\infty} v_n(t)e_n(\hat{Z}_t) + \frac{b-a}{4c} \hat{Z}_t^2 + \frac{b+a}{2} \hat{Z}_t \right\} \\ &= \lim_{T \rightarrow \infty} \frac{1}{T-t} v_0(t)e_0(\hat{Z}_t) \\ &= \frac{b-a}{4c} \lim_{T \rightarrow \infty} \frac{1}{T-t} \int_t^T \sigma^2(s)ds. \end{aligned}$$

This together with Lemma 4.4 leads to the following theorem.

Theorem 4.16 (Log Growth Rate of LP Wealth under Time-Dependent Volatility). *Assuming $\mu_X = \mu_Y = \mu$, the logarithmic growth rate of an LP's wealth in a G3M can be expressed as*

$$\lim_{T \rightarrow \infty} \frac{\mathbb{E}[\ln V_T]}{T} = \mu - \left[\frac{(1-\gamma)w(1-w)}{1-w+\gamma w} + \frac{(1-\gamma)w(1-w)}{\gamma(1-w)+w} \right] \frac{1}{4 \ln \gamma} \lim_{T \rightarrow \infty} \frac{1}{T} \int_0^T \sigma^2(s)ds.$$

This theorem demonstrates how the time-averaged volatility influences the long-term growth of LP wealth. Furthermore, since the volatility process $\tilde{\sigma}_t$ is independent of the mispricing process Z_t , by conditioning on the σ -algebra generated by $\tilde{\sigma}_t$ then applying the tower property for conditional expectation, we obtain the logarithmic growth rate of LP's wealth under driftless, independent stochastic volatility as follows.

Theorem 4.17 (Log Growth Rate under Independent Stochastic Volatility). *Assuming $\mu_X = \mu_Y = \mu$, the logarithmic growth rate of an LP's wealth in a G3M can be expressed as*

$$\begin{aligned} & \lim_{T \rightarrow \infty} \frac{\mathbb{E}[\ln V_T]}{T} \\ &= \mu - \left[\frac{(1-\gamma)w(1-w)}{1-w+\gamma w} + \frac{(1-\gamma)w(1-w)}{\gamma(1-w)+w} \right] \frac{1}{4 \ln \gamma} \lim_{T \rightarrow \infty} \frac{1}{T} \int_0^T \mathbb{E}[\tilde{\sigma}_s^2] ds. \end{aligned}$$

We conclude the section by showing that if the stochastic but independent drift and volatility converge to their corresponding L^2 limits, similar asymptotics in expectation as in Corollary 4.14 can also be obtained.

Theorem 4.18 (Log Growth Rate of LP Wealth in G3M Independent Volatility and Drift). *Assume that the mispricing process Z_t follows the reflected diffusion process in the interval $[-c, c]$ governed by*

$$dZ_t = \tilde{\mu}_t dt + \tilde{\sigma}_t dW_t + dL_t - dU_t, \quad (57)$$

where the coefficients $\tilde{\sigma}_t$ and $\tilde{\mu}_t$ are stochastic but independent of the driving Brownian motion W_t . Further, assume that the limits of the coefficients $\tilde{\sigma}_t$ and $\tilde{\mu}_t$ as t approaches infinity exist almost surely and in L^2 . Specifically, there exists an $\epsilon > 0$ such that

$$\lim_{t \rightarrow \infty} \tilde{\sigma}_t^2 = \sigma^2 \geq \epsilon, \quad \lim_{t \rightarrow \infty} \tilde{\mu}_t = \mu \quad (58)$$

almost surely and in L^2 , where μ and σ^2 are square integrable random variables. The long-term expected logarithmic growth rate of an LP's wealth in a G3M can be expressed as

$$\lim_{T \rightarrow \infty} \frac{\mathbb{E}[\ln V_T]}{T} = w\mu_X + (1-w)\mu_Y + \frac{(1-\gamma)w(1-w)}{1-w+\gamma w} \alpha + \frac{(1-\gamma)w(1-w)}{\gamma(1-w)+w} \beta,$$

where

$$\alpha = \beta = -\frac{1}{4 \ln \gamma} \mathbb{E}[\sigma^2], \quad \text{if } \theta = 0 \text{ almost surely;}$$

$$\alpha = \mathbb{E}\left[\frac{\mu}{\gamma^{-2\theta} - 1}\right], \quad \beta = \mathbb{E}\left[\frac{\mu}{1 - \gamma^{2\theta}}\right], \quad \text{if } \theta \neq 0,$$

where $\theta = \frac{2\mu}{\sigma^2}$, should the expectations exist.

Proof. The proof essentially is based on conditioning on the realizations of $\tilde{\mu}_t$ and $\tilde{\sigma}_t$ followed by applying the tower property since $\tilde{\mu}$ and $\tilde{\sigma}$ are independent of the Brownian motion W_t . \square

We remark that the long-term expected logarithmic growth rate considered in Theorem 4.18 can also be obtained differently by first calculating the condition expectations as in (34), then apply the asymptotic result given in Corollary 4.14. This route is applicable even when $\tilde{\mu}_t$ and $\tilde{\sigma}_t$ are not independent of W_t ; it is, however, subject to the determination of the conditional expectations in (34), which in general do not admit easy-to-access analytical expressions. The expression obtained in Theorem 4.18 is more tractable in that it is subject to the determination of the limiting distributions for μ and σ^2 as well as the corresponding expectations. However, it applies only if $\tilde{\mu}_t$ and $\tilde{\sigma}_t$ are independent of W_t .

CONCLUSION

This paper investigated the growth of liquidity provider (LP) wealth in Geometric Mean Market Makers (G3Ms), explicitly considering the impacts of continuous-time arbitrage and transaction fees. We extended the analysis of arbitrage in LP profitability beyond the constant product models studied in [TW20] to encompass a broader class of G3Ms.

Our model-free approach, which builds on the framework in [MMRZ22b, MMRZ22a, MMR23], provides a refined understanding of G3M dynamics under the influence of arbitrage and fees. A key result is our characterization of LP wealth growth through a stochastic model driven by the mispricing process between the G3M and an external reference market. This model elucidates the crucial role of trading fees in LP returns and demonstrates how arbitrage activity establishes a no-trading band around the reference market price.

Our analysis reveals that the adverse selection risk posed by arbitrageurs necessitates a nuanced understanding of LP wealth dynamics. Notably, we demonstrated that, under certain market conditions, G3Ms with fees can outperform both buy-and-hold and constant rebalanced portfolio strategies. This finding highlights the potential of G3Ms as a competitive investment product within the DeFi landscape, effectively functioning as on-chain index funds.

Several promising avenues for future research emerge from our work. These include incorporating noise trader order flows to create more realistic market dynamics, investigating the interplay between different AMM liquidity pools, refining LP wealth growth models to account for factors like impermanent loss, and extending the analysis to G3Ms with dynamic weights, drawing connections to stochastic portfolio theory (SPT) as explored in [Eva21, Fer02, KF09]. These research directions will further enrich our understanding of AMM functionality and its broader implications for liquidity providers and the DeFi ecosystem.

ACKNOWLEDGEMENT

The authors express their sincere gratitude to Shuenn-Jyi Sheu for his invaluable insights and guidance throughout this research. We also appreciate the fruitful discussions and support from our colleagues, which significantly contributed to the development of this work. We are also grateful to the anonymous referee for their careful reading of the manuscript and their constructive comments and suggestions, which helped improve the quality of this paper.

S.-N. T. gratefully acknowledges the financial support from the National Science and Technology Council of Taiwan under grant 111-2115-M-007-014-MY3. Furthermore, S.-N. T. extends heartfelt thanks to Ju-Yi Yen for her unwavering encouragement and support, which were instrumental in making this collaborative effort possible.

C. Y. Lee was supported in part by a research startup fund of the Chinese University of Hong Kong, Shenzhen and the Shenzhen Peacock fund 2025TC0013.

APPENDIX A. UNIQUENESS FOR THE FOKKER-PLANCK EQUATION

Here we provide details for the uniqueness of solutions p and \hat{p} in the proof of Lemma 4.3. Let $q(t, z) = p(t, z) - \hat{p}(t, z)$. Then q solves the PDE

$$\begin{cases} q_t = -(\mu q)_z + \frac{1}{2}(\sigma^2 q)_{zz}, & t > 0, z \in (-c, c), \\ \mu q - \frac{1}{2}(\sigma^2 q)_{zz} = 0 & \text{at } z = \pm c, \\ q(0, z) = 0 & z \in [-c, c]. \end{cases} \quad (59)$$

We use the energy method to show that $q = 0$. Let

$$E(t) = \frac{1}{2} \int_{-c}^c q^2(t, z) dz.$$

Using the PDE in (59), integrating by parts, and taking into account the boundary condition in (59), we have for any $t \in [0, T]$ that

$$\begin{aligned} E'(t) &= \int_{-c}^c q q_t dz = - \int_{-c}^c q (\mu q)_z dz + \frac{1}{2} \int_{-c}^c q (\sigma^2 q)_{zz} dz \\ &= \int_{-c}^c \mu q q_z dz - \frac{1}{2} \int_{-c}^c q_z (\sigma^2 q)_z dz \\ &= \int_{-c}^c (\mu - \sigma \sigma_z) q q_z dz - \frac{1}{2} \int_{-c}^c \sigma^2 (q_z)^2 dz. \end{aligned}$$

By assumption, μ , σ and σ_z are bounded. Moreover, by the strong ellipticity (39) of σ and Young's inequality, we deduce that for some $C > 0$,

$$\begin{aligned} E'(t) &\leq C \int_{-c}^c |q| |q_z| dz - \frac{\varepsilon}{2} \int_{-c}^c (q_z)^2 \\ &\leq \frac{C^2}{2\varepsilon} \int_{-c}^c q^2 dz + \frac{\varepsilon}{2} \int_{-c}^c (q_z)^2 - \frac{\varepsilon}{2} \int_{-c}^c (q_z)^2 dz \\ &\leq \frac{C^2}{2\varepsilon} \int_{-c}^c q^2 dz = \frac{C^2}{\varepsilon} E(t). \end{aligned}$$

Hence, Gronwall's inequality implies that $E(t) \leq e^{(C^2/\varepsilon)t} E(0) = 0$ for any $t \in [0, T]$. This shows that $p(t, \cdot) = \hat{p}(t, \cdot)$.

APPENDIX B. STURM-LIOUVILLE THEORY

This section provides a brief overview of Sturm-Liouville theory, which plays a key role in analyzing the mispricing process and deriving the growth rate of LP wealth in our framework.

B.1. Eigensystem. Consider a second-order differential operator \mathcal{L} in the Sturm-Liouville form

$$\mathcal{L}u = \frac{1}{\omega(x)} \frac{d}{dx} \left(p(x) \frac{du}{dx} \right), \quad (60)$$

where $\omega(x)$ and $p(x)$ are smooth functions. Let $(\lambda_n, e_n(x))$ represent the eigensystem of \mathcal{L} , satisfying

$$\mathcal{L}e_n(x) = -\lambda_n e_n(x) \quad \text{for } n \geq 0,$$

with Neumann boundary conditions $e'_n(-c) = e'_n(c) = 0$ on the interval $[-c, c]$. These boundary conditions correspond to reflecting boundaries for the associated diffusion process. Since a constant function always satisfies the equation with $\lambda_0 = 0$, the first normalized eigenfunction is $e_0 \equiv \frac{1}{K}$, where $K = (\int_{-c}^c \omega(x)dx)^{\frac{1}{2}}$.

The eigensystem possesses the following important properties:

- $\lambda_n > 0$ for all $n \in \mathbb{N}_{>0}$ and each eigenvalue is of multiplicity one.
- The normalized eigenfunctions e_n form an orthonormal basis for the space $L^2[-c, c]$ with respect to the weight function $\omega(x)$. This means

$$\int_{-c}^c e_n(x) e_m(x) \omega(x) dx = \delta_{nm}$$

where δ_{nm} is the Kronecker delta. Consequently, any function $f \in L^2[-c, c]$ can be expressed as

$$f(x) = \sum_{n=0}^{\infty} \xi_n e_n(x),$$

where the coefficients ξ_n are given by

$$\xi_n = \int_{-c}^c f(x) e_n(x) \omega(x) dx.$$

This expansion converges in the L^2 sense with respect to the weight function $\omega(x)$.

B.2. Solution to inhomogeneous PDE with general terminal condition. For the inhomogeneous parabolic PDE

$$u_t + \mathcal{L}u + f(x) = 0 \quad (61)$$

with terminal condition $u(T, x) = g(x)$ and Neumann boundary conditions $u_x(t, -c) = u_x(t, c) = 0$ for $t < T$, we show how to formulate its solution using the eigensystem given in Section B.1. Let the eigenfunction expansions for functions f and g be represented as

$$f(x) = \sum_{n=0}^{\infty} \xi_n e_n(x), \quad g(x) = \sum_{n=0}^{\infty} \eta_n e_n(x)$$

where the coefficients ξ_n and η_n are defined as:

$$\xi_n = \int_{-c}^c f(x) e_n(x) \omega(x) dx, \quad \eta_n = \int_{-c}^c g(x) e_n(x) \omega(x) dx.$$

In particular, the term ξ_0 , expressed as

$$\xi_0 = \frac{\int_{-c}^c f(x) \omega(x) dx}{\int_{-c}^c \omega(x) dx}, \quad (62)$$

is the weighted average of f over the interval $[-c, c]$, weighted by ω .

The solution to the terminal-boundary value problem (61) can be expressed in terms of eigenvalues and eigenfunctions for \mathcal{L} as

$$u(t, x) = \xi_0(T - t) + \eta_0 + \sum_{n=1}^{\infty} \left\{ \frac{\xi_n}{\lambda_n} [1 - e^{-\lambda_n(T-t)}] + \eta_n e^{-\lambda_n(T-t)} \right\} e_n(x). \quad (63)$$

Consequently, the following long-term time-averaged limit of u exists

$$\lim_{T \rightarrow \infty} \frac{u(t, x)}{T - t} = \xi_0,$$

where recall that ξ_0 , given in (62), is the zeroth Fourier coefficient of the inhomogeneous term f . We note that this long-term time-averaged limit depends only on the zeroth coefficient of the inhomogeneous term; no other higher-order coefficients are involved. Furthermore, we have the following long-term limit of u as $T \rightarrow \infty$

$$\lim_{T \rightarrow \infty} \{u(t, x) - \xi_0(T - t)\} = \eta_0 + \sum_{n=1}^{\infty} \frac{\xi_n}{\lambda_n} e_n(x).$$

B.3. Transition density in terms of eigensystem. The following proposition shows that the transition density of a reflected diffusion (35) within a bounded interval can be expressed in terms of the eigensystem of its infinitesimal generator with Neumann boundary conditions.

Proposition B.1. *The transition density p of a reflected diffusion in the interval $[-c, c]$ with infinitesimal generator \mathcal{L} given in (60) can be expressed in terms of the eigensystem for \mathcal{L} as*

$$p(T, y|t, x) = \sum_{n=0}^{\infty} e^{-\lambda_n(T-t)} e_n(x) e_n(y) \omega(y).$$

This leads to the following characterization of the steady-state distribution:

Theorem B.2 (Steady-State Distribution). *The reflected diffusion within the interval $[-c, c]$ with infinitesimal generator (60) has a steady-state distribution π given by*

$$\pi(dx) = \frac{\omega(x)}{\int_{-c}^c \omega(\xi) d\xi} dx, \quad x \in [-c, c].$$

Proof. By Proposition B.1, as $T \rightarrow \infty$, the steady-state distribution is given by

$$\begin{aligned} \lim_{T \rightarrow \infty} p(T, y|t, x) &= \lim_{T \rightarrow \infty} \sum_{n=0}^{\infty} e^{-\lambda_n(T-t)} e_n(x) e_n(y) \omega(y) \\ &= e_0(x) e_0(y) \omega(y) = \frac{\omega(y)}{\int_{-c}^c \omega(x) dx} \end{aligned}$$

since the zeroth eigenfunction $e_0(x)$ is a constant $e_0(x) = \left(\int_{-c}^c \omega(\xi) d\xi\right)^{-\frac{1}{2}}$. \square

APPENDIX C. TIME-INHOMOGENEOUS REFLECTED DIFFUSION

In this appendix, we provide the proof of the long-term time averaged expectation of a time-inhomogeneous reflected diffusion as stated in Theorem 4.13. For fixed t, x , we shall sometimes suppress the reference to t, x in the transition density p and simply denote $p(s, y|t, x)$ by $p(s, y)$ for simplicity. For any function φ defined in $[-c, c]$, $\|\varphi\|_2$ denotes the L^2 norm of φ in $[-c, c]$. We start with stating an estimate of the L^2 -norm between the transition density p and the stationary density q in the following lemma, whose proof is

omitted (for interested readers, we refer it to, for instance, [Kah83], see (3.21) on P.276), is classical and crucial to the proof that follows.

Lemma C.1. *Assume that the infinitesimal generator operator $\mathcal{L}_t := \frac{\sigma^2(t,x)}{2} \partial_x^2 + \mu(t,x) \partial_x$ is strongly elliptic, i.e., there exists an $\epsilon > 0$ such that $\sigma(t,x) \geq \epsilon$ for all t, x , and that the coefficients σ and μ are smooth and bounded, the following estimates hold. For any $T > t$, we have*

$$\|p(T, \cdot | t, x) - q\|_2 \leq \frac{C}{\sqrt{T-t}} \quad (64)$$

for some constant C depending only on the interval $[-c, c]$. As a result, we note that the L^2 norm of $p(s, y)$ is bounded above by

$$\|p(s, \cdot)\|_2 \leq \|p(s, \cdot) - q\|_2 + \|q\|_2 \leq \frac{C}{\sqrt{s-t}} + \|q\|_2 \quad (65)$$

for $s > t$.

With Lemma C.1 in hand, we provide the proof of Theorem 4.13 as follows. Note that we have

$$\begin{aligned} u(t, x) &= \mathbb{E} \left[g(X_T) + \int_t^T f(s, X_s) ds \mid \hat{Z}_t = x \right] \\ &= \int_{-c}^c g(y) p(T, y | t, x) dy + \int_t^T \int_{-c}^c f(s, y) p(s, y | t, x) dy ds \end{aligned}$$

since p is the transition density. Consider

$$\frac{u(t, x)}{T-t} = \frac{1}{T-t} \int_{-c}^c g(y) p(T, y | t, x) dy + \frac{1}{T-t} \int_t^T \int_{-c}^c f(s, y) p(s, y | t, x) dy ds, \quad (66)$$

We separately determine the limits of the two terms on the right-hand side of (66).

For the first term in (66), by applying the Cauchy-Schwarz inequality we obtain that, for $T \geq t$,

$$\left| \int_{-c}^c g(y) p(T, y | t, x) dy \right| \leq \|g\|_2 \|p(T, \cdot | t, x)\|_2 \leq \|g\|_2 \left\{ \frac{C}{\sqrt{T-t}} + \|q\|_2 \right\}$$

where in the second inequality, we applied the upper bound for $p(T, \cdot)$ given in (65). It follows that

$$\lim_{T \rightarrow \infty} \frac{1}{T-t} \left| \int_{-c}^c g(y) p(T, y | t, x) dy \right| \leq \lim_{T \rightarrow \infty} \frac{\|g\|_2}{T-t} \left\{ \frac{C}{\sqrt{T-t}} + \|q\|_2 \right\} = 0. \quad (67)$$

For the second term in (66), we claim that, as $\lim_{t \rightarrow \infty} f(t, x) = \bar{f}(x)$ in L^2 , we have

$$\lim_{T \rightarrow \infty} \frac{1}{T-t} \int_t^T \int_{-c}^c f(s, y) p(s, y | t, x) dy ds = \int_{-c}^c \bar{f}(y) q(y) dy \quad (68)$$

for every t and x . Note that by applying the Cauchy-Schwarz inequality, we have

$$\begin{aligned} & \left| \int_{-c}^c \{f(s, y)p(s, y) - \bar{f}(y)q(y)\} dy \right| \\ & \leq \int_{-c}^c |f(s, y) - \bar{f}(y)| p(s, y) dy + \int_{-c}^c |\bar{f}(y)| |p(s, y) - q(y)| dy \\ & \leq \|f(s, \cdot) - \bar{f}\|_2 \|p(s, \cdot)\|_2 + \|\bar{f}\|_2 \|p(s, \cdot) - q\|_2. \end{aligned} \quad (69)$$

We shall deal with the two pieces in (69) separately. For the first piece, since $f(s, y) \rightarrow \bar{f}(y)$ as $s \rightarrow \infty$ in L^2 , for any $\epsilon > 0$, there exists a $t_1 \geq t$ such that

$$\|f(s, \cdot) - \bar{f}\|_2 < \epsilon$$

for all $s > t_1$. Hence, for given $T > t_1$ we have

$$\begin{aligned} & \int_t^T \|f(s, \cdot) - \bar{f}\|_2 \|p(s, \cdot)\|_2 ds \\ &= \int_t^{t_1} \|f(s, \cdot) - \bar{f}\|_2 \|p(s, \cdot)\|_2 ds + \int_{t_1}^T \|f(s, \cdot) - \bar{f}\|_2 \|p(s, \cdot)\|_2 ds \\ &\leq M \int_t^{t_1} \left\{ \frac{C}{\sqrt{s-t}} + \|q\|_2 \right\} ds + \epsilon \int_{t_1}^T \left\{ \frac{C}{\sqrt{s-t}} + \|q\|_2 \right\} ds \\ &= M \{2C\sqrt{t_1-t} + \|q\|_2(t_1-t)\} + \epsilon \{2C\sqrt{T-t_1} + \|q\|_2(T-t_1)\}, \end{aligned}$$

where in the inequality we applied the upper bound for p given in (65) and the constant $M > 0$ is defined as

$$\infty > M := \max_{t \leq s \leq t_1} \|f(s, \cdot)\|_2 + \|\bar{f}\|_2 \geq \|f(s, \cdot)\|_2 + \|\bar{f}\|_2 \geq \|f(s, \cdot) - \bar{f}\|_2.$$

It follows that

$$\begin{aligned} & \lim_{T \rightarrow \infty} \frac{1}{T-t} \int_t^T \|f(s, \cdot) - \bar{f}\|_2 \|p(s, \cdot)\|_2 ds \\ &\leq \lim_{T \rightarrow \infty} \frac{M}{T-t} \{2C\sqrt{t_1-t} + \|q\|_2(t_1-t)\} + \lim_{T \rightarrow \infty} \frac{\epsilon}{T-t} \{2C\sqrt{T-t_1} + \|q\|_2(T-t_1)\} \\ &= \epsilon \|q\|_2. \end{aligned}$$

Since $\epsilon > 0$ is arbitrary, we obtain the limit of time-average of the first piece in (69) as T approaches infinity as

$$\lim_{T \rightarrow \infty} \frac{1}{T-t} \int_t^T \|f(s, \cdot) - \bar{f}\|_2 \|p(s, \cdot)\|_2 ds = 0.$$

Next, for the second piece in (69), note that from (64) we have

$$\int_t^T \|p(s, \cdot) - q\|_2 ds \leq \int_t^T \frac{C}{\sqrt{s-t}} ds = 2C\sqrt{T-t}.$$

It follows immediately that

$$\lim_{T \rightarrow \infty} \frac{1}{T-t} \int_t^T \|\bar{f}\|_2 \|p(s, \cdot) - q\|_2 ds \leq 2C \lim_{T \rightarrow \infty} \frac{\|\bar{f}\|_2}{T-t} \sqrt{T-t} = 0.$$

Finally, by combining (67) and (68) we conclude that

$$\lim_{T \rightarrow \infty} \frac{1}{T-t} u(t, x) = \int_{-c}^c \bar{f}(y) q(y) dy.$$

REFERENCES

- [AC20] Guillermo Angeris and Tarun Chitra. Improved price oracles: Constant function market makers. In *Proceedings of the 2nd ACM Conference on Advances in Financial Technologies (AFT '20)*, AFT '20, pages 80–91, New York, NY, USA, 2020. Association for Computing Machinery.
- [AKC⁺19] Guillermo Angeris, Hsien-Tang Kao, Rei Chiang, Charlie Noyes, and Tarun Chitra. An analysis of uniswap markets. *arXiv e-prints*, 2019.
- [AZR20] Hayden Adams, Noah Zinsmeister, and Dan Robinson. Uniswap v2 core, 2020.
- [Bas98] Richard F. Bass. *Diffusions and elliptic operators*. Probability and its Applications (New York). Springer-Verlag, New York, 1998.
- [BEK24] W. Brönnimann, P. Egloff, and T. Krabichler. Automated market makers and their implications for liquidity providers. *Digital Finance*, 6:573–604, 2024.
- [CDM23] Álvaro Cartea, Fayçal Drissi, and Marcello Monga. Predictable losses of liquidity provision in constant function markets and concentrated liquidity markets. *Applied Mathematical Finance*, 30(2):69–93, 2023.
- [CDM24] Álvaro Cartea, Fayçal Drissi, and Marcello Monga. Decentralized finance and automated market making: Predictable loss and optimal liquidity provision. *SIAM Journal on Financial Mathematics*, 15(3):931–959, 2024.
- [CJ21] Agostino Capponi and Ruizhe Jia. The adoption of blockchain-based decentralized exchanges. *arXiv e-prints*, 2021.
- [Eva21] Alex Evans. Liquidity provider returns in geometric mean markets. *Cryptoeconomic Systems*, 1(2), October 2021.
- [Fer02] E. Robert Fernholz. *Stochastic Portfolio Theory*, volume 48 of *Applications of Mathematics (New York)*. Springer-Verlag, New York, 2002.
- [FMW23] Masaaki Fukasawa, Basile Maire, and Marcus Wunsch. Weighted variance swaps hedge against impermanent loss. *Quantitative Finance*, 23(6):901–911, 2023.
- [FMW24] Masaaki Fukasawa, Basile Maire, and Marcus Wunsch. Model-free hedging of impermanent loss in geometric mean market makers with proportional transaction fees. *Applied Mathematical Finance*, 31(2):108–129, 2024.
- [GM23] Emmanuel Gobet and Anastasia Melachrinos. Decentralized finance & blockchain technology. In *SIAM Financial Mathematics and Engineering 2023*, Philadelphia, United States, 2023.
- [GW13] Peter Glynn and Rob Wang. Central limit theorems and large deviations for additive functionals of reflecting diffusion processes. *Fields Institute Communications*, 76, 2013.
- [Gyö86] I. Gyöngy. Mimicking the one-dimensional marginal distributions of processes having an Itô differential. *Probability Theory and Related Fields*, 71(4):501–516, 1986.
- [Har13] J. Michael Harrison. *Brownian Models of Performance and Control*. Cambridge University Press, Cambridge, 2013.
- [Kah83] Charles S. Kahane. On the asymptotic behavior of solutions of parabolic equations. *Czechoslovak Mathematical Journal*, 33(2):262–285, 1983.
- [KF09] Ioannis Karatzas and Robert Fernholz. Stochastic portfolio theory: an overview. In Alain Bensoussan and Qiang Zhang, editors, *Special Volume: Mathematical Modeling and Numerical Methods in Finance*, volume 15 of *Handbook of Numerical Analysis*, pages 89–167. Elsevier, 2009.
- [Kry85] N. V. Krylov. Once more about the connection between elliptic operators and Itô's stochastic equations. In *Statistics and control of stochastic processes (Moscow, 1984)*, Transl. Ser. Math. Engrg., pages 214–229. Optimization Software, New York, 1985.
- [KS91] Ioannis Karatzas and Steven E. Shreve. *Brownian motion and stochastic calculus*, volume 113 of *Graduate Texts in Mathematics*. Springer-Verlag, New York, second edition, 1991.

- [LS84] P.-L. Lions and A.-S. Sznitman. Stochastic differential equations with reflecting boundary conditions. *Communications on Pure and Applied Mathematics*, 37(4):511–537, 1984.
- [MM19] Fernando Martinelli and Nikolai Mushegian. Balancer: A non-custodial portfolio manager, liquidity provider, and price sensor, 2019.
- [MMR23] Jason Milionis, Ciamac C. Moallemi, and Tim Roughgarden. Automated market making and arbitrage profits in the presence of fees. *arXiv e-prints*, 2023.
- [MMRZ22a] Jason Milionis, Ciamac C. Moallemi, Tim Roughgarden, and Anthony Lee Zhang. Automated market making and loss-versus-rebalancing. *arXiv e-prints*, 2022.
- [MMRZ22b] Jason Milionis, Ciamac C. Moallemi, Tim Roughgarden, and Anthony Lee Zhang. Quantifying loss in automated market makers. In *Proceedings of the 2022 ACM CCS Workshop on Decentralized Finance and Security (DeFi'22)*, pages 71–74, New York, NY, USA, 2022. Association for Computing Machinery.
- [Moh22] V. Mohan. Automated market makers and decentralized exchanges: a defi primer. *Financial Innovation*, 8(20), 2022.
- [NTYY24] Joseph Najnudel, Shen-Ning Tung, Kazutoshi Yamazaki, and Ju-Yi Yen. An arbitrage driven price dynamics of automated market makers in the presence of fees. *Frontiers of Mathematical Finance*, 3(4):560–571, 2024.
- [RY99] Daniel Revuz and Marc Yor. *Continuous martingales and Brownian motion*, volume 293 of *Grundlehren der mathematischen Wissenschaften*. Springer-Verlag, Berlin, third edition, 1999.
- [TW20] Martin Tassy and David White. Growth rate of a liquidity provider's wealth in $xy = c$ automated market makers, 2020.

CHEUK YIN LEE

SCHOOL OF SCIENCE AND ENGINEERING,
THE CHINESE UNIVERSITY OF HONG KONG, SHENZHEN
SHENZHEN, CHINA

Email address: leechuekyin@cuhk.edu.cn

SHEN-NING TUNG

DEPARTMENT OF MATHEMATICS,
NATIONAL TSING HUA UNIVERSITY
HSINCHU, TAIWAN

Email address: tung@math.nthu.edu.tw

TAI-HO WANG

DEPARTMENT OF MATHEMATICS
BARUCH COLLEGE, THE CITY UNIVERSITY OF NEW YORK
1 BERNARD BARUCH WAY, NEW YORK, NY10010

Email address: tai-ho.wang@baruch.cuny.edu

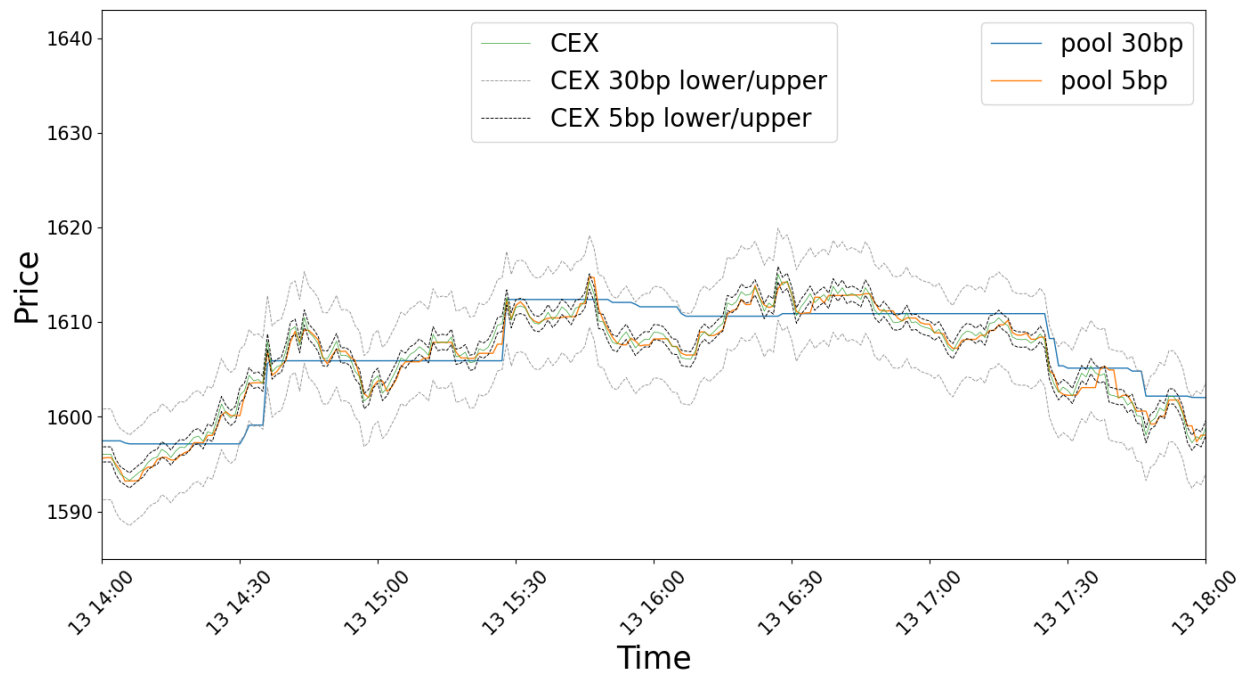


FIGURE 1. Price time series (1-minute intervals) from 14:00:00 to 18:00:00 on September 13, 2023. Dashed lines indicate the upper and lower boundaries of the no-arbitrage region.

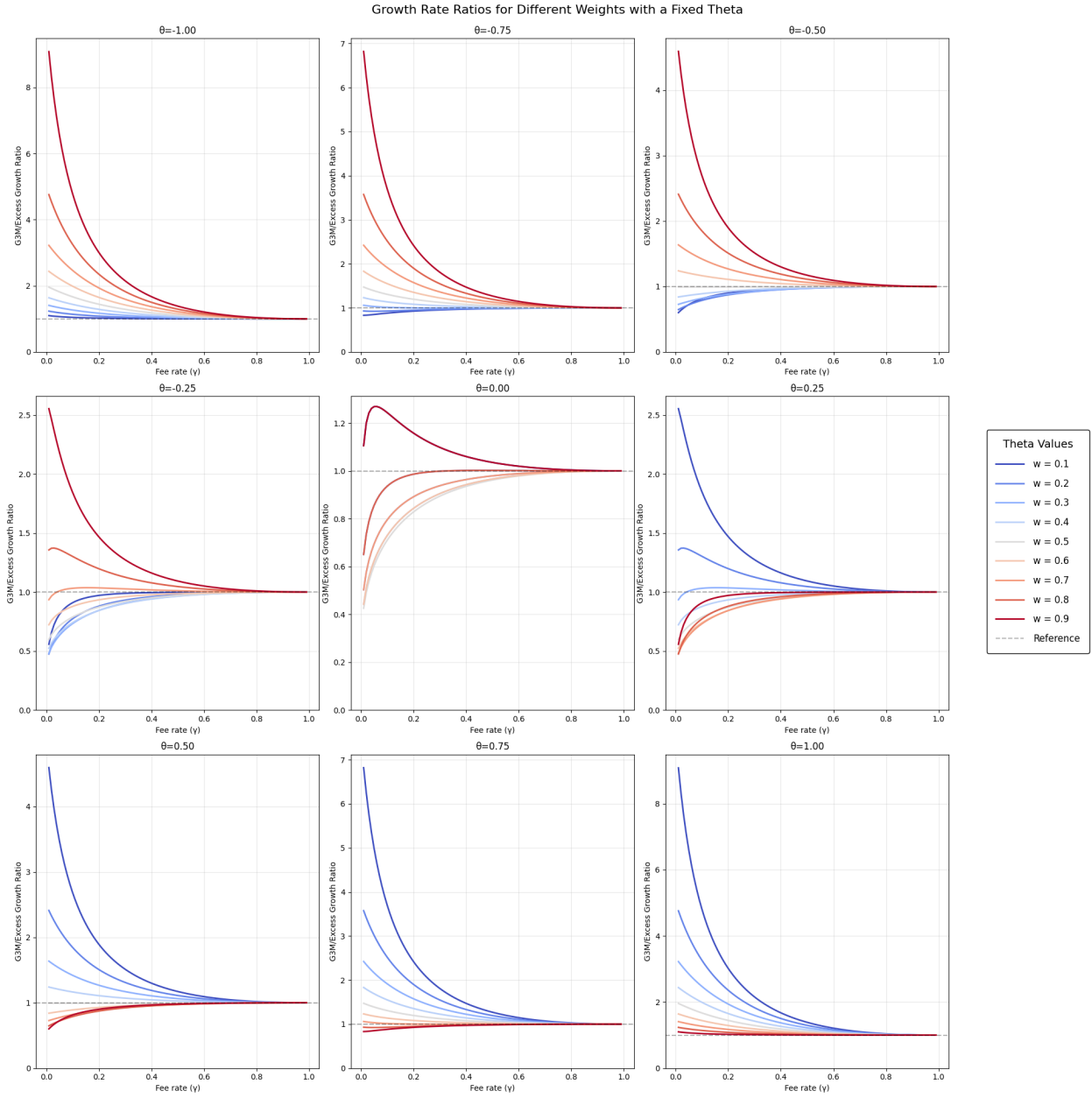


FIGURE 2. Growth rate ratio for different values of weights. Note the symmetry between positive and negative θ values.

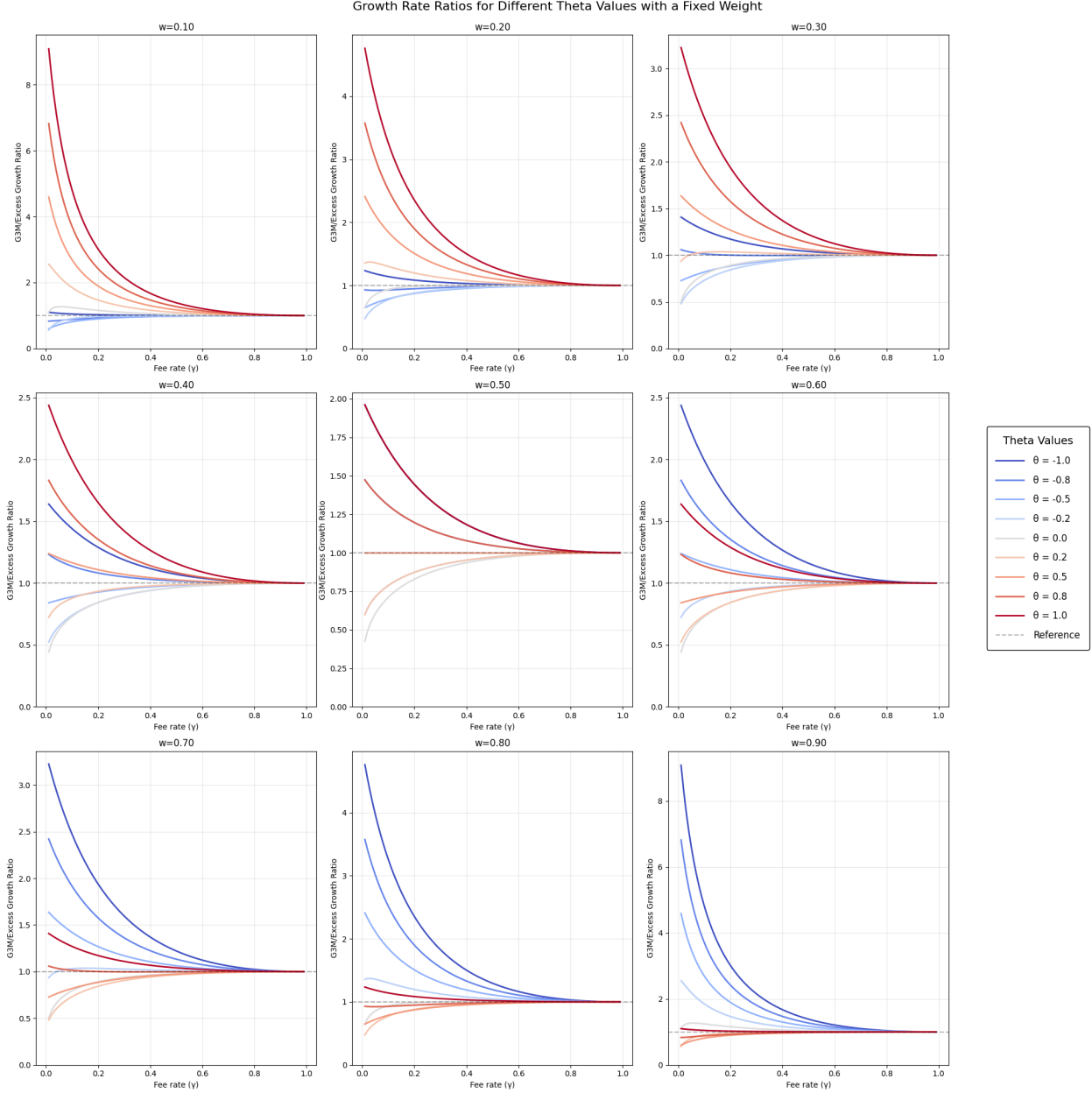


FIGURE 3. Growth rate ratio for different values of θ . Note the symmetry around $w = \frac{1}{2}$.

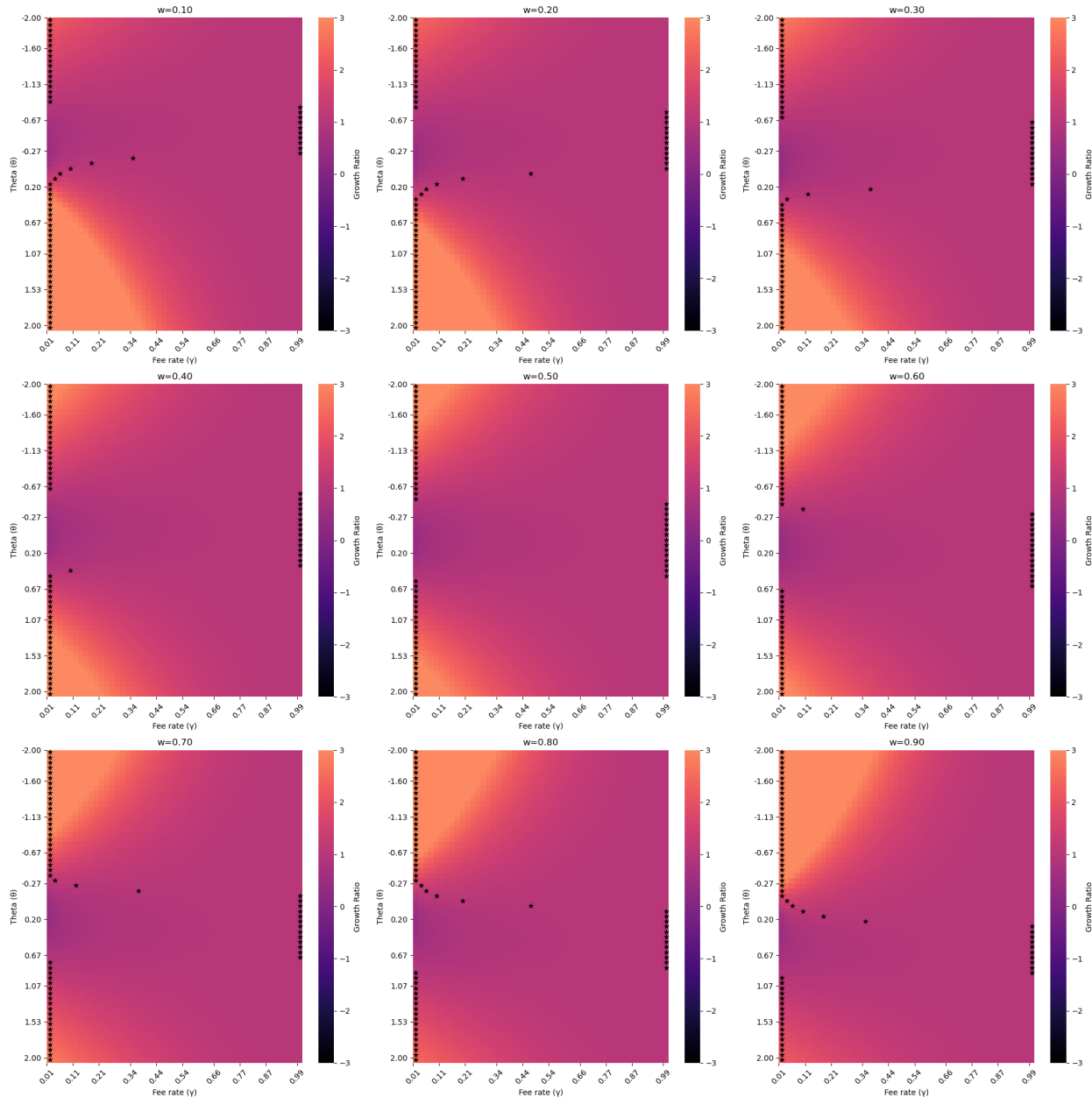


FIGURE 4. Heatmap of growth rate ratio for different weights, with maximum values labeled.

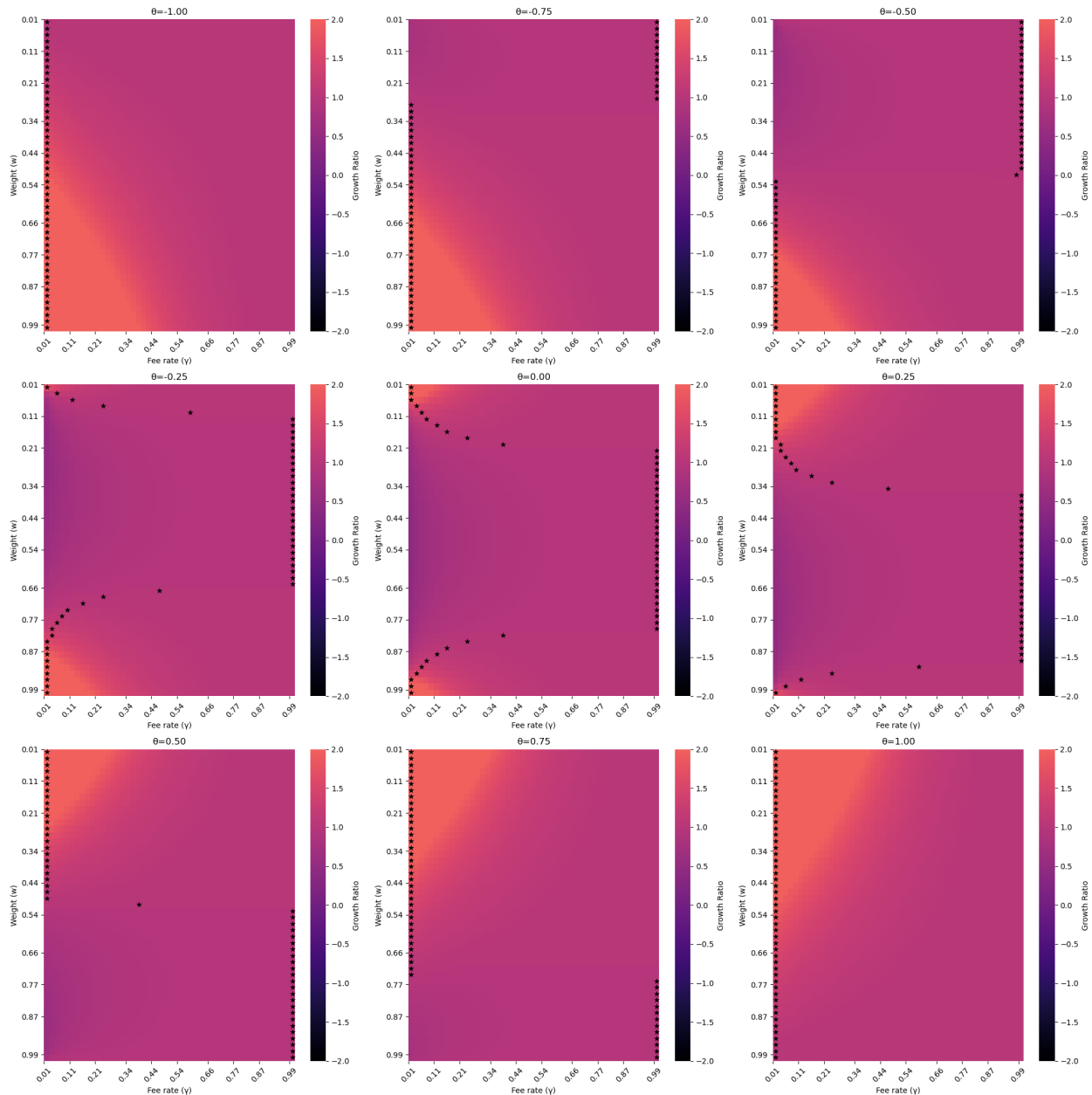


FIGURE 5. Heatmap of growth rate ratio for different values of θ , with maximum values labeled.